arXiv:cond-mat/0001380v1 [cond-mat.stat-mech] 26 Jan 2000

Semiclassical Time Evolution of the Density Matrix and Tunneling

Joachim Ankerhold and Hermann Grabert
Fakultät für Physik, Albert-Ludwigs-Universität Freiburg, Hermann-Herder-Straße 3, D-79104 Freiburg, Germany
(February 1, 2008)

The time dependent density matrix of a system with potential barrier is studied using path integrals. The characterization of the initial state, which is assumed to be restricted to one side of the barrier, and the time evolution of the density matrix lead to a three-fold path integral which is evaluated in the semiclassical limit. The semiclassical trajectories are found to move in the complex coordinate plane and barrier penetration only arises due to fluctuations. Both the form of the semiclassical paths and the relevant fluctuations change significantly as a function of temperature. The semiclassical analysis leads to a detailed picture of barrier penetration in the real time domain and the changeover from thermal activation to quantum tunneling. Deep tunneling is associated with quasi-zero modes in the fluctuation spectrum about the semiclassical orbits in the long time limit. The connection between this real time description of tunneling and the standard imaginary time instanton approach is established. Specific results are given for a double well potential and an Eckart barrier.

PACS numbers:03.65.Sq,82.20.Db,05.40.+j

I. INTRODUCTION

Semiclassical theories have been found extremely powerful in understanding the dynamics of complex quantum mechanical systems. Special attention has been paid to theories of tunneling processes as they occur in physics, chemistry, and biology. Currently, a variety of quantum rate theories are in use explaining experimental findings for several situations of interest [1]. Thereby, roughly speaking, two different strategies can be distinguished. The first class of approaches constructs the rate from purely thermodynamic considerations. An example is the bounce or instanton method (also called ImF method), originated by Langer [2] and extended by several authors [3]. In essence, tunneling rates are derived from the imaginary time dynamics in the inverted potential. Other approaches of this type [4,5] start from periodic orbit theory [6] in imaginary time. Tractable rate formulae are obtained with the centroid method [7] leading to a semi-empirical separation of dynamical and thermal factors. These methods are computationally very efficient and have been applied successfully to systems as diverse as tunneling centers in metals, Josephson junctions, or hydrogen bonds, to name but a few. However, closer examination reveals that these theories are based in one way or another on *ad hoc* assumptions that are not derived from first principles. For instance, the ImF method postulates a relation between the decay rate and the imaginary part of the free energy. In fact, in some cases thermodynamic methods fail to predict the correct rate, e.g. they do not reproduce the energy diffusion limited decay for very weakly damped systems at finite temperature. Moreover, these methods are designed to describe incoherent decay only.

The second class of theories describes barrier crossing in terms of dynamical quantities. Perhaps most familiar is Yamamoto's rate formula [8], in essence a Kubo type formula relating the rate with a flux-flux correlation function. As shown in [9] it is exact only for scattering problems, while in multi- or metastable systems one has to assume the existence of a plateau region for times long compared to typical relaxation times but small compared to decay times. This restricts the approach to incoherent decay. Recent advances in the real time description of barrier crossing based on flux-flux correlations were made e.g. by Voth *et al.* [10], who incorporated analytically known dynamical factors into the rate expressions. Quite recently, Pollak and coworkers [11,12] were able to improve this idea by using a thermally symmetrized flux operator. A different way of including dynamical information in an approximate way, favored by Miller and coworkers, employs semiclassical Initial Value Representation (IVR) for the quantum propagator [13]. Although quite successful at high to moderate temperatures, where the quantum dynamics is governed by quasi-classical above-barrier processes, these approaches usually fail at low temperatures where deep tunneling prevails. Finally, we mention a kind of hybrid approach, the "real time" instanton theory [14] which includes tunneling in the real time propagator by means of instantaneous tunneling transitions. This method is restricted to multi-stable systems in the low temperature limit [15]. Hence, although the semiclassical theory of quantum tunneling is often regarded to be well settled, this turns out to be true only for some limiting cases. What would be desirable is a

semiclassical theory starting from first principles that covers the entire range of temperatures as well as coherent and incoherent tunneling processes.

In the realm of classical physics the theory of thermally activated rates is rather firmly based. In a seminal paper [16] Kramers determined thermal decay rates from the equation of motion for the phase space distribution function, i.e., from the real time dynamics of the system. A corresponding treatment of tunneling in the semiclassical limit seems not to be possible, since all real time minimal action paths connecting two sides of the barrier have energies *larger* than the barrier energy. In the dynamical approaches discussed above these trajectories do account for tunneling corrections to classical rates [13,17], but it is usually argued [18,19] that within a semiclassical theory deep tunneling can only be described by incorporating in addition imaginary time trajectories as they are used in thermodynamic methods. The lack of a first principles semiclassical theory of tunneling is intimately connected with a fundamental shortcoming of semiclassical real time propagators derived from a single dominant path. Since tunneling arises from coherent interference of waves, a satisfactory semiclassical theory needs to capture this interference pattern in terms of an appropriate family of real time paths rather than making *ad-hoc* modifications of simple semiclassical propagators.

Very recently, we have proposed a theory for transport across a barrier based solely on the real time dynamics of the density matrix and the semiclassical approximation [20]. As a notable feature, the method applies equally well to damped and undamped systems and comprises in a unified way the entire range from thermally activated decay to low temperature tunneling. In appropriate limits the results of other methods are recovered. Here, we explain the technicalities of the approach and evaluate the semiclassical propagator in detail for two paradigmatic systems, namely, a double well potential and an Eckart barrier. Thereby, we mainly concentrate on one-dimensional models. It turns out that the corresponding theory already reveals the basic structure and that the generalization to multidimensional systems, though tedious in detail, is straightforward within the path integral formalism [21].

The article is organized as follows. Next, in Sec. II, we outline the general semiclassical theory which is then used in Sec. III to derive as a simple example the stationary flux across a parabolic barrier. The main part of the paper studies the real time dynamics from high down to vanishing temperature for the cases of a double well potential (Sec. IV) and an Eckart barrier (Sec. V). Finally, in Sec. VI we summarize the main features of the approach and present our conclusions.

II. GENERAL THEORY

We consider a statistical ensemble of quantum mechanical particles of mass M moving in a barrier potential $V(q)$ at inverse temperature $\beta = 1/k_{\rm B}T$. We chose the coordinate q so that the barrier top is located at $q = 0$ and measure energies relative to the barrier energy by putting $V(0) = 0$. The initial nonequilibrium state is assumed to be of the form of an equilibrium state restricted to the left side of the barrier. Below we will invoke the semiclassical approximation which is appropriate provided the barrier height V_b is by far the largest energy scale in the system. The time evolution of the density matrix $\rho(t) = \exp(-iHt/\hbar)\rho(0)\exp(iHt/\hbar)$ reads in coordinate representation

$$\rho(q_f, q_f', t) = \int dq_i dq_i' G_t(q_f, q_i)\rho(q_i, q_i', 0)G_t(q_f', q_i')^* \tag{1}$$

where the real-time propagator is given by

$$G_t(q, q') = \langle q|\exp(-iHt/\hbar)|q'\rangle \tag{2}$$

and $\rho(q_i, q_i', 0)$ describes the initial state. In principle, for our purpose any initial distribution that matches onto equilibrium on the left side and vanishes on the right side of the barrier top is appropriate. As long as the restricted equilibrium state gives vanishing probability to find the particle on the right side of the barrier top, different initial preparations lead to the same long time behavior of the density matrix. Here we put explicitly

$$\rho(q, q', 0) = Z^{-1}\rho_\beta(q, q')\theta(-q)\theta(-q') \tag{3}$$

for convenience with the proper normalization factor Z and the equilibrium density matrix

$$\rho_\beta(q, q') = \langle q|\exp(-\beta H)|q'\rangle. \tag{4}$$

Now, employing the path integral representation for $\exp(\pm itH/\hbar)$ and $\exp(-\beta H)$, respectively, the above integrand in Eq. (1) can be written as a three-fold path integral where two real time paths $q(u)$ and $q'(u)$ run in the interval $0 \le u \le t$ from q_i and q_i' to fixed endpoints q_f and q_f', respectively, while those former coordinates are connected by

an imaginary time path $\bar{q}(\sigma)$ in the interval $0 \leq \sigma \leq \hbar\beta$, see fig. 1. The real time paths describe the time evolution of the system and the imaginary time path the initial state. Of course, a more complete theory would explicitly include the coupling to a heat bath environment. In fact, the general scheme of this approach in the case of damped systems has already been given elsewhere [21]. Much of the analysis presented below can in principle be extended to this situation, however, only a limited number of steps can be carried out analytically due to the more complicated form of the effective action functionals. Here, we limit ourselves to undamped motion which allows to treat deep tunneling without resorting to numerical methods. This way, the guiding concepts will become more transparent.

The density matrix $\rho(q, q', t)$ contains all information about the nonequilibrium quantum process, in particular, the average of the operator $F = [p\delta(q) + \delta(q)p]/2M$ gives the flux out of the metastable state, i.e., in coordinate representation

$$J(t) = (\hbar/2iM)\,[\partial\rho(q_f, -q_f, t)/\partial q_f]_{q_f=0}. \tag{5}$$

If the flux becomes quasi-stationary, $J(t) = J_{\rm fl}$ within a certain "plateau region" of time, the escape rate follows from $\Gamma = J_{\rm fl}$.

While an exact solution of Eq. (1) for anharmonic barrier potentials is not possible, a high barrier naturally suggests a semiclassical approximation. In the semiclassical limit the above path integrals are dominated by minimal action paths determined by Hamilton's equation of motion either in the potential $V(q)$ (for the real time propagators) or $-V(q)$ (for the equilibrium density matrix). Each path contributes with an exponential factor containing its minimal action and a prefactor arising from the Gaussian fluctuations about the minimal action paths. Specifically, the action in real time reads

$$S(q, q') = \int_0^t du[M\dot{q}^2/2 - V(q)] \tag{6}$$

while its imaginary time version, the so-called Euclidian action, is given by

$$\bar{S}(q, q') = \int_0^{\hbar\beta} d\sigma[M\dot{\bar{q}}^2/2 + V(\bar{q})]. \tag{7}$$

Thus, in the Gaussian semiclassics the propagator (2) is approximated as

$$G_t(q, q') = \sum_{\rm cl.paths} \sqrt{A(q, q')}\, \exp\left[\frac{i}{\hbar}S(q, q') - i\frac{\pi}{2}\nu\right] \tag{8}$$

where $A(q, q') = [-\partial^2 S(q, q')/\partial q\partial q']/2\pi i\hbar$ and ν is the Maslov index. Throughout this paper we also use an equivalent representation of the prefactor, namely,

$$A(q, q') = \frac{iM}{2\pi\hbar}\,\left[\dot{q}(0)\dot{q}(t)\frac{\partial^2 W(q, q')}{\partial E^2}\right]^{-1} \tag{9}$$

where $W(q, q') = \int_q^{q'} dq'' p = S(q, q') + Et$ is the short action. The corresponding approximation to the equilibrium density matrix (4) follows by formal analytic continuation $t \to -i\hbar\beta$, i.e., by replacing $S(q, q')$ by $i\bar{S}(q, q')$ in Eq. (8) with $\nu = 0$. As a result, the integrand in Eq. (1) is completely determined by classical mechanics in real and imaginary time, respectively, and dominated by an action factor $\exp[-\Sigma(q_f, q'_f|q_i, q'_i)/\hbar - i\pi(\nu - \nu')/2]$ with

$$\Sigma(q_f, q'_f|q_i, q'_i) = -iS(q_f, q_i) + \bar{S}(q_i, q'_i) + iS(q'_f, q'_i). \tag{10}$$

With the approximate integrand at hand, it is consistent to evaluate the ordinary integrations in Eq. (1) in stationary phase. The stationary phase points are determined by minimizing Σ with respect to the initial coordinates q_i, q'_i, i.e.,

$$\left.\frac{\partial\Sigma}{\partial q_i}\right|_{(q_f, q'_f)} = 0, \qquad \left.\frac{\partial\Sigma}{\partial q'_i}\right|_{(q_f, q'_f)} = 0. \tag{11}$$

Since the endpoints q_f, q'_f are fixed, the resulting stationary phase points $q_s(t)$ and $q'_s(t)$ are functions of time with $q_s(0) = q_f$, $q'_s(0) = q'_f$. For finite t these roots are in general complex. The dominant imaginary time path $\bar{q}_s(\sigma)$ connects $q'_s(t)$ with $q_s(t)$, and the two real time paths $q(u)$ and $q'(u)$ connect $q_s(t)$ and $q'_s(t)$ with q_f and q'_f, respectively.

Hence, the steepest–descent approximation naturally provides a mapping from the integration contour in the complex time plane onto a loop in the complex coordinate space connecting the endpoints [fig. 1]. To avoid potential confusion with other methods, we emphasize that the appearance of complex paths has nothing to do with tunneling but rather is merely a consequence of the stationary phase approximation and holds also for systems with no barrier at all. In fact, it turns out that the complex semiclassical real-time trajectories used here never cross the barrier top, in contrast to paths emerging from *ad hoc* complexification procedures occasionally adopted to describe barrier penetration [22].

Starting from the steepest descent conditions (11) and exploiting Hamilton-Jacobi mechanics, one immediately derives

$$p_s(0) = i\bar{p}_s(\hbar\beta)\ ,\ p'_s(0) = i\bar{p}_s(0)\ ,\ E = E' = \bar{E}. \tag{12}$$

Here, $p_s(u)$ $[p'_s(u)]$ is the momentum of the real time path $q(u)$ $[q'(u)]$ with energy E $[E']$ connecting q_s $[q'_s]$ and q_f $[q'_f]$; accordingly, $\bar{p}_s(\sigma)$ denotes the momentum of the imaginary time path $\bar{q}_s(\sigma)$ running from q'_s to q_s with Euclidian energy $\bar{E} = -\bar{p}_s^2/2M + V(\bar{q})$, see fig. 1. Eq. (12) can also be expressed as $d\Sigma/dt = 0$ with the solution

$$\Sigma(q_f, q'_f|q_s, q'_s) = \bar{S}(q_f, q'_f). \tag{13}$$

Hence along the loop of steepest descent paths the full action is just given by the equilibrium action and thus independent of time. Differentiating Eq. (13) with respect to q_f, q'_f, one finds

$$p_s(t) = i\bar{p}_0(\hbar\beta), \quad p'_s(t) = i\bar{p}_0(0) \tag{14}$$

where $\bar{p}_0(\sigma)$ is now the momentum of the imaginary time path $\bar{q}_0(\sigma)$ connecting q'_f with q_f in imaginary time $\hbar\beta$. This path has Euclidean energy $\bar{E}_f$ which depends on q_f, q'_f and $\hbar\beta$ but not on t. Hence, we first deduce that the energies in Eq. (12) are given by $\bar{E}_f$, which implies energy and momentum conservation throughout the loop in fig. 1. Secondly, we arrive at the remarkable result that the sequence of time-dependent stationary phase points $q_s(t)$ $[q'_s(t)]$ is itself a minimal action path starting at $q_s(0) = q_f$ $[q'_s(0) = q'_f]$ with energy $\bar{E}_f$.

To complete the ordinary integrations in Eq. (1) over the initial coordinates q_i, q'_i we transform to fluctuations $y = q_i - q_s$ and $y' = q'_i - q'_s$ about the stationary phase points. An expansion of the full action (10) for fixed endpoints q_f, q'_f around the stationary phase points up to second order leads to $\Sigma(q_f, q'_f|q_i, q'_i) = \bar{S}(q_f, q'_f) + \delta\Sigma^{(2)}(y, y')$ with

$$\delta^{(2)}\Sigma(y, y') = \frac{1}{2}\ (y, y')\ \Sigma^{(2)}\ \begin{pmatrix} y \\ y' \end{pmatrix} \tag{15}$$

where

$$\Sigma^{(2)} = \begin{pmatrix} \Sigma_{ss}\Sigma_{ss'} \\ \Sigma_{ss'}\Sigma_{s's'} \end{pmatrix} \tag{16}$$

is the matrix of second order derivatives, $\Sigma_{ss} = \partial^2\Sigma(q_i, q'_i)/\partial q_i^2$ etc., to be taken at $q_i = q_s, q'_i = q'_s$.

Inserting Eq. (3) into Eq. (1), the integrand now reduces to a product of Gaussian weight factors for deviations from the stationary phase points and an initial state factor $\theta(-q_s - y)\theta(-q'_s - y')$ describing deviations from thermal equilibrium at $t = 0$. Provided there is only one semiclassical path for each of the propagators, we obtain from Eq. (1) by virtue of Eqs. (13) and (15) the semiclassical time dependent density matrix in the form

$$\rho(q_f, q'_f, t) = \frac{1}{Z}\rho_\beta(q_f, q'_f)\, g(q_f, q'_f, t). \tag{17}$$

Here, deviations from equilibrium are described by a "form factor"

$$g(q_f, q'_f, t) = \frac{1}{\pi}\int_{-\infty}^{u(q_s)} dz \int_{-\infty}^{u'(z,q'_s)} dz'\, \mathrm{e}^{-(z^2+z'^2)}, \tag{18}$$

where

$$u(q_s) = -q_s\sqrt{\frac{\mathrm{Det}[\Sigma^{(2)}]}{2\hbar\Sigma_{s's'}}}, \quad u'(q'_s, z) = -q'_s\sqrt{\frac{\Sigma_{s's'}}{2\hbar}} + z\frac{\Sigma_{ss'}}{\sqrt{\mathrm{Det}[\Sigma^{(2)}]}} \tag{19}$$

with $\mathrm{Det}[\Sigma^{(2)}] = \Sigma_{ss}\Sigma_{s's'} - (\Sigma_{ss'})^2$. In deriving Eq. (17) we invoked that Hamilton Jacobi mechanics implies [23]

$$\left[\frac{A(q_f,q_s)\bar{A}(q_s,q_s')A(q_f',q_s')}{\mathrm{Det}[\Sigma^{(2)}]}\right]^{1/2} = \bar{A}(q_f,q_f'). \tag{20}$$

Note that for an initial equilibrium state, formally $\theta(\cdot)\to 1$ in Eq. (3) so that $u,u'\to\infty$ in Eq. (18), the form factor becomes 1 and the semiclassical density matrix is in fact stationary. If there is more than one classical path one has to sum in Eq. (17) over the contributions of all of them. Certainly, the above formulae (18) and (19) are only applicable as long as the Gaussian semiclassical and stationary phase approximations are valid, i.e. as fluctuations are sufficiently small. This will be seen to be no longer the case for low temperatures and/or very long times. How the classical paths in the complex plane can then be used as a skeleton for an extended semiclassical/stationary phase calculation will be shown below.

In the remaining parts of the article we apply the general formalism to specific barrier potentials. Thereby, since we are particularly interested in the flux across the barrier, we restrict our investigation to non-diagonal end-coordinates q_f and $q_f'=-q_f$ close to the barrier top. This does not mean that we may constrain ourselves to study only local dynamics near the barrier top. Especially for lower temperatures, the nonequilibrium state in the barrier region is predominantly governed by global properties of the potential.

III. PARABOLIC BARRIER

The semiclassical and the stationary phase approximations are always exact for quadratic potentials. Hence, as a simple test case we consider first a parabolic barrier

$$V(q) = -\frac{1}{2}M\omega_b^2\, q^2. \tag{21}$$

Accordingly, the imaginary time dynamics runs in a harmonic oscillator potential. For the minimal action path $\bar{q}_0(\sigma)$ connecting $-q_f$ with q_f in time $\hbar\beta$ one obtains

$$\bar{q}_0(\sigma) = \frac{q_f}{\sin(\omega_b\hbar\beta/2)}\,\sin\left[\omega_b(\sigma-\hbar\beta/2)\right]. \tag{22}$$

This leads to the well-known equilibrium density matrix

$$\rho_\beta(q_f,-q_f) = \frac{1}{\sqrt{4\pi\delta_b^2\sin(\omega_b\hbar\beta)}}\;\exp\left[-\cot(\omega_b\hbar\beta/2)\,\frac{q_f^2}{2\delta_b^2}\right] \tag{23}$$

with the relevant length scale $\delta_b=\sqrt{\hbar/2M\omega_b}$.

The real-time dynamics simply follows. The classical real-time paths $q(u)$ and $q'(u)$ lead to the endpoints q_f and $-q_f$, respectively, and hence obey $q(t)=q_f$, $q'(t)=-q_f$. On the other hand, the stationary phase condition (12) implies $\dot{q}(t)=i\dot{\bar{q}}(\hbar\beta)$, $\dot{q}'(t)=i\dot{\bar{q}}(0)$ and we readily find $q(u)=\bar{q}(\hbar\beta-it+iu)$, i.e.,

$$\begin{aligned} q(u) &= \frac{q_f}{\sin(\omega_b\hbar\beta/2)}\,\sin\left[\omega_b(\hbar\beta/2-it+iu)\right],\\ q'(u) &= q(u+i\hbar\beta),\quad 0\le u\le t. \end{aligned} \tag{24}$$

At time t the imaginary time path $\bar{q}_0(\sigma)$ from $-q_f$ to q_f is mapped onto the path $\bar{q}_s(\sigma)=q(i\hbar\beta-i\sigma), 0\le\sigma\le\hbar\beta$ connecting $q_s'(t)=q'(0)$ with $q_s(t)=q(0)$ (fig. 2). The stationary phase points

$$\begin{aligned} q_s(t) &= \frac{q_f}{\sin(\omega_b\hbar\beta/2)}\sin\left[\omega_b(\hbar\beta/2-it)\right]\\ q_s'(t) &= -q_s(t)^* \end{aligned} \tag{25}$$

are as functions of t also classical paths moving away from the barrier top as t increases – $q_s(t)$ to the right and $q_s'(t)$ to the left for $q_f>0$. For longer times $\omega_b t\gg 1$, the stationary phase points asymptotically tend towards the limiting trajectories starting from $q_f=0$ referred to as asymptotes henceforth. Similar to separatrices in classical phase space, these asymptotes divide the complex plane in regions of negative and positive Euclidian energy: in the sectors including the real axis classical real time motion has $\bar{E}<0$ (but $E\le 0$ or $E>0$) while in the remaining parts

$\bar{E} > 0$. However, in contrast to simple classical separatrices the asymptotes are temperature dependent. The angel α of the q_s and q'_s-asymptotes with the positive and negative real axis, respectively, is found as

$$\alpha = \frac{\pi - \omega_b \hbar \beta}{2}. \tag{26}$$

Now, for the nonequilibrium preparation (3) the initial coordinates q_i, q'_i are constrained to $\mathrm{Re}\{q_i\}$, $\mathrm{Re}\{q'_i\} \leq 0$. Since $q_s(t)$ and $q'_s(t)$ are on different sides of the barrier, $\rho(q_f, -q_f, t)$ gains nonvanishing values *only due to fluctuations* that effectively shift q_i away from q_s and across the barrier top [see Eq. (19)]. For the parabolic barrier potential the matrix elements in (16) take the simple form

$$\begin{aligned} \Sigma_{ss} &= M\omega_b \left[\cot(\omega_b \hbar \beta) - i \coth(\omega_b t)\right], \quad \Sigma_{s's'} = \Sigma^*_{ss}, \\ \Sigma_{ss'} &= -\frac{M\omega_b}{\sin(\omega_b \hbar \beta)} \end{aligned} \tag{27}$$

so that the matrix $\Sigma^{(2)}$ can easily be diagonalized. One finds for the eigenvalues

$$\frac{\lambda_\pm}{M\omega_b} = \cot(\omega_b \hbar \beta) \pm \left[\cot(\omega_b \hbar \beta)^2 - \frac{1}{\sinh(\omega_b t)^2}\right]^{1/2}. \tag{28}$$

While, in principle, with Eq. (18) we can now evaluate the complete dynamics of the density matrix, we will concentrate here on the long time asymptotics of the nonequilibrium state. Then, in the asymptotic region $\omega_b t \gg 1$ the eigenvalue λ_- tends to zero as $\lambda_- \propto M\omega_b \exp(-\omega_b t)$, reflecting the instability of the parabolic barrier. Hence, fluctuations around the stationary phase points with the least action increase occur in the direction of the eigenvector with eigenvalue λ_-. These fluctuations are of the form $y_i = |y_i| \exp[i(\alpha + \omega_b \hbar \beta)]$ and $y'_i = |y_i| \exp(i\alpha)$ so that q_i and q'_i move simultaneously along their asymptotes meeting at the barrier top (see fig. 2). Now, inserting the matrix elements (27) and the stationary phase points (25) into Eq. (19) and considering the limit $\omega_b t \gg 1$, the relevant form factor turns out to be stationary

$$g_{\mathrm{fl}}(q, -q) = \frac{1}{\sqrt{\pi}} \int_{-\infty}^{i2q\Omega} dx \ \mathrm{e}^{-x^2} \tag{29}$$

with $\Omega = \sqrt{\cot(\omega_b \hbar \beta/2)/(8\delta_b^2)}$. The corresponding constant flux across the barrier is obtained from Eqs. (5) and (17) as

$$J_{\mathrm{fl}} = \frac{\hbar}{2ZM} \rho_\beta(0,0) \left.\frac{\partial g_{\mathrm{fl}}(q_f, -q_f)}{\partial q_f}\right|_{q_f = 0} \tag{30}$$

which leads to the well-known result

$$\Gamma = J_{\mathrm{fl}} = \frac{\omega_b}{4\pi} \frac{1}{Z \sin(\omega_b \hbar \beta/2)}. \tag{31}$$

Here, Z denotes an appropriate normalization constant which cannot be derived from the pure parabolic potential. This is not really a problem since realistic potentials always exhibit a well-behaved potential minimum and then Z follows e.g. as the relative normalization with respect to this minimum. Note that for the quadratic potential the results (29) and (31) are formally valid for all times $\omega_b t \gg 1$. However, it was shown in [24] that due to the lack of a well-behaved ground state it makes physically only sense to use the parabolic barrier in $T > T_c$ where $\omega_b \hbar / k_{\mathrm{B}} T_c = \pi$. For lower temperatures $\omega_b \hbar \beta \to \pi$ large quantum fluctuations render the Gaussian approximation insufficient. Interestingly, the rate expression (31) diverges at the lower temperature $T_0 = T_c/2$ only where the parabolic density matrix (23) ceases to exist.

IV. DOUBLE WELL POTENTIAL

A model well-behaved for the entire range of temperatures with many applications is the bistable dynamics of a particle moving in a double well potential

$$V(q) = -\frac{M\omega_b^2}{2}\, q^2 \left[1 - \frac{q^2}{2q_a^2}\right] \tag{32}$$

Here, the barrier is located at $q = 0$, the wells at $q = \pm q_a$, and the barrier height is $V_b = -V(q_a) = (M\omega_b^2/4)q_a^2$. This potential exhibits rich quantum dynamics, namely, incoherent hopping between the wells over a broad range of temperatures that changes to coherent oscillations for $T \to 0$. Due to the complexity of the dynamics this is a highly nontrivial problem for the semiclassical approach where the ratio δ_b/q_a serves as the small parameter.

A. Thermal equilibrium

The Euclidian mechanics in the inverted potential $-V(q)$ can be solved exactly using Jacobian elliptic functions [25]. For the general solution one obtains

$$\bar{q}_0(q_f, \sigma) = B\,\mathrm{sn}\left[\omega(B)\sigma - \phi_f | m\right], \quad 0 \le \sigma \le \hbar\beta \tag{33}$$

where the boundary conditions $\bar{q}_0(q_f, 0) = -q_f$ and $\bar{q}_0(q_f, \hbar\beta) = q_f$ fix the amplitude B and phase ϕ_f. Since the potential is no longer purely quadratic – depending on temperature – there may be several solutions each of them with another amplitude. In Eq. (33) the frequency is given by

$$\omega(B) = \omega_b\, \sqrt{1-\eta^2}, \quad \eta^2 = \frac{B^2}{2q_a^2}, \tag{34}$$

and the phase can be represented as an incomplete elliptic integral

$$\phi_f = F(q_f/B|m) = \int_0^{q_f/B} dx \frac{1}{\sqrt{(1-x^2)(1-mx^2)}} \tag{35}$$

with the so-called modul $m = \eta^2/(1-\eta^2)$. From the boundary condition $\bar{q}_0(\hbar\beta) = -\bar{q}_0(0)$ and the periodicity of the Jacobian function, $\mathrm{sn}[z + 2rK(m)|m] = (-1)^r \mathrm{sn}[z|m], r = 1, 2, 3, \ldots$ with $K(m) = F(1, m)$, the amplitude B is determined by

$$\omega(B)\hbar\beta = 2rK(m) + \left[1 + (-1)^r\right]\phi_f. \tag{36}$$

Since $K(m), \phi_f > 0$, for fixed $\omega_b\hbar\beta$ real solutions to this equation exist only for a finite number of integers $r \ge 0$.

Let us briefly discuss the trajectories $\bar{q}_0(q_f, \sigma)$ as the temperature is lowered. For high temperatures only solutions of Eq. (36) with $r = 0$ exist corresponding to direct paths from $-q_f$ to q_f; particularly, $\bar{q}_0(0, \sigma) = 0$. As the temperature drops below the critical temperature

$$T_c = \hbar\omega_b/\pi k_\mathrm{B}, \tag{37}$$

i.e. $\omega_b\hbar\beta > \pi$, solutions of Eq. (36) with $r = 1$ arise. Then, for $q_f = 0$ the barrier top can be joined with itself also by two nonlocal paths denoted by $\bar{q}_\pm(0, \sigma)$ oscillating in $-V(q)$ to the right and to the left with amplitudes $\pm q_1$, respectively, and energy $\bar{E}_1 = V(q_1)$. With further decreasing temperature q_1 grows and eventually saturates at q_a for $T \to 0$. For finite q_f the situation is rather similar: oscillating paths $\bar{q}_\pm(q_f, \sigma)$ exist for all $q_f < q_1$. These paths connect $-q_f$ with q_f via a turning point at $\pm q_1$, thus, differing from $\bar{q}_\pm(0, \sigma)$ only by a phase shift. The described scenario repeats in an analog way at all $T = T_c/r, r = 2, 3, 4, \ldots$, where r counts the number of turning points. At zero temperature all these oscillating paths reach $\pm q_a$ with the same energy $\bar{E}_a = V(q_a)$ and are then called instantons.

Now that all proper Euclidian trajectories are identified, the semiclassical equilibrium state follows readily. For high temperatures $T > T_c$ and end-coordinates q_f near the barrier top, $\rho_\beta(q_f, -q_f)$ basically coincides with the parabolic result (23) and anharmonic corrections are negligible. This situation changes drastically for temperatures near T_c. Then, the bifurcation of new classical paths leads to large quantum fluctuations and one has to go beyond the Gaussian approximation of the fluctuation integral. Slightly below T_c a caustic appears for $q_f = q_1$. Since the region around T_c was already studied in detail elsewhere [24] we omit here this crossover region and proceed with temperatures sufficiently below T_c where near the barrier top Gaussian semiclassics is again applicable. It turns out that the paths newly emerging near T_c are stable and dominate $\rho_\beta(q, q')$ for all $T_c > T > 0$ while the unstable "high temperature" path and those springing up at lower T give negligible contributions. Since for $q_f < q_1$ all paths $\bar{q}_\pm(q_f, \sigma)$ differ only by a phase shift, one has for the corresponding actions

$$\bar{S}_{\pm}(q_f,-q_f)=\bar{S}_{+}(0,0)=\bar{S}_{-}(0,0) \tag{38}$$

so that

$$\rho_\beta(q_f,-q_f)=2[\bar{A}(q_f,-q_f)]^{1/2}\exp[-\bar{S}_{+}(0,0)/\hbar],\quad q_f<q_1. \tag{39}$$

Accordingly, the matrix element $\rho_\beta(q_f,-q_f)$ changes to a non-Gaussian distribution with a local minimum at $q_f=0$ and two maxima at $q_f=\pm q_1$. Thereby $\bar{S}_{+}(0,0)<0$, so that the probability $\rho_\beta(0,0)$ to find the particle at $q=0$ is substantially enhanced compared to its classical value.

For $T\to 0$ it is no longer sufficient to include only the trajectories with $r=1$ in the semiclassical analysis but rather all other paths with $r>1$ must also be taken into account. This is due to the fact that the smaller action factors of these latter paths are compensated for by zero mode phase factors from the corresponding fluctuation path integrals. Accordingly, all instanton contributions are summed up to yield e.g. for coordinates near the barrier top

$$\rho_\beta(q_f,-q_f)=\frac{8}{\delta_a\sqrt{2\pi}}\,\mathrm{e}^{-\beta[V(q_a)+\hbar\omega_a/2]-\bar{W}_a/\hbar}\left[\cosh\left(\frac{\hbar\beta\Delta}{2}\right)+\cosh\left(\frac{q_fq_a}{2\delta_a^2}\right)\sinh\left(\frac{\hbar\beta\Delta}{2}\right)\right]. \tag{40}$$

Here, $\bar{W}_a\equiv\bar{W}(-q_a,q_a)=-\hbar\beta\bar{E}+\bar{S}(-q_a,q_a)$ is the short action for an instanton from $-q_a$ to q_a. Further,

$$\Delta=\omega_a\frac{4q_a}{\sqrt{2\pi}\delta_a}\;\exp(-\bar{W}_a/\hbar) \tag{41}$$

denotes the WKB tunnel splitting with the well frequency $\omega_a=\omega_b\sqrt{2}$ and $\delta_a^2=\hbar/2M\omega_a$.

B. Dynamics of stationary phase points

As in case of the parabolic barrier, the stationary real-time paths can be directly infered from the Euclidian dynamics at $t=0$. From Eq. (33) and the stationary phase condition we have

$$q_s(t)=B\,\mathrm{sn}[\phi_f-i\omega(B)t|m],\qquad q_s'(t)=-q_s[(-1)^{r+1}t] \tag{42}$$

and $\bar{q}_0(\sigma)$ is mapped at time t onto $\bar{q}_s(\sigma)=\bar{q}_0[\sigma+i(-1)^{r+1}t]$ where r follows from Eq. (36). In the sequel we always formulate the semiclassical theory in terms of the real time paths q_s,q_s' that "start" at the endpoints $q_f,-q_f$, respectively, and reach the initial points q_i,q_i' after time t. Since the endpoints $q_f,-q_f$ are fixed, while the most relevant initial coordinates depend on time, this backward view of the dynamics is in fact more transparent. The real time trajectories now start from the end coordinates we are interested in and lead to the relevant initial coordinates that need to be integrated over with an integrand weighted according to the initial deviations from equilibrium. The path $q_s(t)$ runs in the complex coordinate plane as a periodic orbit with period $t_p(q_f)=2K(1-m)/\omega(B)$ (fig. 3). Within one period it connects q_f with q_f via a loop crossing the real axis also after time $t_p(q_f)/2$ at the point $q_c(q_f)=q_s[q_f,t_p(q_f)/2]\geq q_a$. Thus $q_s(t)$ stays always on the same side of the barrier top and likewise $q_s'(t)$ on the other side so that the complex dynamics of the stationary phase points starting from q_f and $-q_f$, respectively, reflects a bounded motion in either of the potential wells.

Let us consider the stationary orbits as the temperature decreases. For high temperatures $T>T_c$, i.e. $r=0$, each q_f-dependent loop carries its own period $t_p(q_f)$ and energy $E(q_f)$. If $q_f\neq 0$, t_p is small for $T\gg T_c$ and the real time dynamics corresponds to a fast bouncing back and forth in the well. As the temperature is lowered the period grows while simultaneously the "width" of the loop $q_c(q_f)$ shrinks. In the special case $q_f=0$ the real time path reduces to a constant $q_s(0,t)=0$. For temperatures $T<T_c$ the situation changes according to the appearence of new oscillating Euclidian paths $\bar{q}_{\pm}(q_f,\sigma)$ for $q_f<q_1$. In contrast to the high temperature case *all* stationary phase point paths with $q_f<q_1$ have then the same period $t_p(q_f)=t_p(q_1)$ and energy $E(q_f)=\bar{E}_1$, and differ only in their respective phases. Special cases are $q_f=0$ and $q_f=q_1$: The path $q_s(q_f,t),q_f\to 0$ runs along the imaginary axis, while the orbit $q_s(q_1,t)$ degenerates to a usual well oscillation along the real axis. These properties have a direct effect on the corresponding actions. One finds by employing Cauchy's theorem that after each period

$$S[q_s(q_f,nt_p),q_f]=S[q_s(q_1,nt_p),q_1],\quad q_f\leq q_1. \tag{43}$$

Hence, all $q_s(q_f,t)$ for $q_f<q_1$ can be seen as phase shifted copies of the specific real path $q_s(q_1,t)$ having the same energy, period, and action increase during one period. In particular, the period $t_p(q_1)$ is large for $T\lesssim T_c$ when q_1 is still small, $t_p(q_1)\approx\ln(q_a/q_1)/\omega_b$, and drops down to $t_p(q_a)=2\pi/\omega_a$ in the limit $T\to 0$.

C. Nonequilibrium dynamics for high and moderately low temperatures

For $t = 0$ the density matrix is given by the initial state (3). The semiclassical time evolution of this state follows by inserting the proper classical paths into Eq.(17). In the sequel, we mainly focus on the long time dynamics and are especially interested in a plateau region where the time evolution becomes quasi-stationary.

We start by addressing the question when a plateau region does exist at all. Inserting the classical paths into $g(q_f, -q_f, t)$ in Eq. (19), the detailed analysis reveals that this function becomes stationary when the ratio $q_s(t)/p_s(t)$ reduces to a constant. Since this will only occur within the parabolic barrier region, a least upper bound for a plateau region follows from the time interval within which a particle starting at a typical point q_b near the barrier top continues to experience a nearly parabolic potential. This leads to $t \ll t_p(q_b)$. The lower bound is obvious: it is given by the transient time near the top, i.e. by $1/\omega_b$. Hence, a plateau region can be estimated to occur as long as a there is clear separation of time scales between local barrier motion and global well oscillations, i.e., $1 \ll \omega_b t \ll \omega_b t_p(q_b)$. Particularly, in the temperature domain where a plateau region exists, the Gaussian/stationary phase approximations are valid and we can actually calculate a rate. These approximations break down when the stationary phase points move far from the barrier top and times of order $t_p(q_b)$ become relevant for the barrier crossing. This range will be addressed in the next section.

For high temperatures $T > T_c$ the typical length scale q_b can be identified with $\delta_b = \sqrt{\hbar/2M\omega_b}$. Then, the separation of time scales fails for very high temperatures where $k_{\rm B}T \gtrsim 8V_b$ meaning that the thermal energy is of the same order or larger than the barrier height. With decreasing temperature t_p grows so that for $\omega_b\hbar\beta$ of order 1 a wide plateau range appears with $t_p \approx \ln(q_a/\delta_b)/\omega_b$. In the corresponding density matrix anharmonic corrections are small, and we obtain approximately the parabolic result (29). To get the rate, here, the proper normalization constant Z is taken as the partition function of the harmonic well oscillator

$$Z = \frac{1}{2\sinh(\omega_a\hbar\beta/2)}\,{\rm e}^{\beta V_b}. \tag{44}$$

Hence, from Eq. (30) one regains the known result

$$\Gamma = \frac{\omega_b}{2\pi}\,\frac{\sinh(\omega_a\hbar\beta/2)}{\sin(\omega_b\hbar\beta/2)}\,{\rm e}^{-\beta V_b} \tag{45}$$

with the exponential Arrhenius factor and a characteristic $\hbar$-dependent prefactor that formally tends to ω_a/ω_b in the classical limit and describes the quantum enhancement of the rate as T_c is approached.

At this point we have to be very careful: a detailed analysis [21] of the full density matrix $\rho(q_f, q_f', t)$, not only of its nondiagonal part, reveals that the nonequilibrium effects described by the flux state are restricted to the barrier region only in the presence of damping, consistent with the fact that finite temperature decay rates require coupling to a heat bath. In the absence of damping the full density matrix does not become quasistationary and the real time trajectories explore the strongly anharmonic range of the potential. Hence, an evaluation of the rate based upon a supposedly quasi-stationary flux state $\rho_{\rm fl}(q_f, -q_f)$ for the undamped case corresponds to the transition state theory result. We refer to [21] for a detailed discussion of this point.

As the temperature reaches T_c large quantum fluctuations occur and the impact of anharmonicities becomes substantial. A detailed study of the bifurcation range around T_c is quite tedious and was already presented in [26]. Thus, we omit explicit results here and proceed with temperatures $T \lesssim T_c$ where for coordinates close to the barrier top a Gaussian approximation – then around the newly emerging paths with amplitudes $\pm q_1$ – is again appropriate. As discussed above all real time paths with $q_f < q_1$ have now the same oscillation period $t_p(q_1) \approx \ln(q_a/q_1)/\omega_b$. One observes that even though they are influenced by the anharmonicity of the potential via the Euclidian amplitude q_1, their time evolution for $T \lesssim T_c$ is still dominated by parabolic properties. Then, a somewhat lengthy algebra leads to the quasi-stationary density matrix

$$\rho_{\rm fl}(q_f, -q_f) = \frac{1}{2}\rho_\beta(q_f, -q_f)\left[g_{\rm fl}^{(+)}(q_f, -q_f) + g_{\rm fl}^{(-)}(q_f, -q_f)\right] \tag{46}$$

where $g_{\rm fl}^{(\pm)}$ describe the contributions from each of the two oscillating Euclidian paths. Note that due to symmetry in $\rho_\beta(q_f, -q_f)$, these contributions are identical and just lead to a factor of 2. In the temperature domain studied here, q_1 can be gained analytically from Eq. (36) as

$$q_1 = \frac{2q_a}{\sqrt{3}}\left(1 - \frac{\pi^2}{\omega_b^2\hbar^2\beta^2}\right)^{1/2}. \tag{47}$$

Accordingly, one finds with some algebra for the thermal distribution

$$\rho_\beta(0,0) = \frac{1}{\sqrt{2\pi\delta_b^2|\sin(\omega_b\hbar\beta)|}}\,\exp\left[\frac{\omega_b\hbar\beta q_a^2}{12\delta_b^2}\left(1-\frac{\pi^2}{\omega_b^2\hbar^2\beta^2}\right)^2\right]. \tag{48}$$

The form factor now has two contributions of the form (18) and for $\kappa_1 = \partial\ln(q_1)/\partial(\omega_b\hbar\beta) \gg 1$ the corresponding integration boundaries read

$$u^{(\pm)}(q_f) = \frac{\pm q_1 + iq_f}{4\delta_b\sqrt{\kappa_1}},\quad u'^{(\pm)}(q_f,z) = \kappa_1\left[u^{(\pm)}(q_f) - z\right]. \tag{49}$$

Here, we employed that near T_c the derivative Σ_{ss} is dominated by $\partial^2\bar{S}/\partial q_i^2$ which is proportional to $\partial E_1/\partial(\omega_b\hbar\beta) \propto \kappa_1$. This way, using the normalization (44), the result for the rate is

$$\Gamma = \frac{\omega_b}{2\pi}\frac{\sinh(\omega_a\hbar\beta/2)}{\sqrt{2|\sin(\omega_b\hbar\beta)|}}\sqrt{\omega_b\hbar\beta - \frac{\pi^2}{\omega_b\hbar\beta}}\;\;\mathrm{e}^{-\beta V_b}. \tag{50}$$

This expression is valid for temperatures $T < T_c$ where still $\kappa_1 \gg 1$, a region which can be estimated as T somewhat larger than $T_c/2$. There are two interesting observations to mention: first, the exponentially large term in the thermal distribution (48) – a consequence of the new Euclidian paths – is exactly canceled by a corresponding term which arises from the derivative of the form factor. This way, the rate is still dominated by the characteristic "Arrhenius factor". Second, in the limit $T \to T_c$ the above-T_c formula (45) and the below-T_c result (50) both approach $\Gamma_c = (\omega_b/2\pi)\sinh(\omega_a\hbar\beta/2)\exp(-\beta V_b)$, however, the derivatives $\partial\Gamma/\partial T$ are different. This discontinuity in the slope of the temperature dependent rate is removed by the full semiclassical theory [26] which takes the non-Gaussian fluctuations near T_c into account and leads to a smooth changeover between the rate formulas (45) and (50).

With further decreasing temperature the amplitude q_1 tends to saturate at q_a so that $\kappa_1 \to 0$ and the above rate expression is no longer applicable. Furthermore, the plateau region shrinks and eventually vanishes so that the assumption of a quasistationary flux state becomes inadequate even in the sense of a transition state theory limit of a weak damping theory. We note that in case of finite damping a meaningful rate can be found for much lower temperatures, then describing incoherent quantum tunneling. To investigate the time dependence of $\rho(q_f,-q_f,t)$ with no damping in the limit of deep tunneling, we consider the case $T = 0$ in the next section.

D. Nonequilibrium dynamics for zero temperature

Any Gaussian semiclassics to the real time propagator is expected to break down for very low temperatures and very long times where quantum tunneling comes into play. In fact, as yet no satisfactory semiclassical procedure was found to describe deep tunneling in the time domain. The crucial question thereby is: how can classical trajectories that either oscillate in one of the potential wells, here with energy $E < 0$, or move over the barrier, here with $E > 0$, produce exponentially small contributions to the semiclassical propagator which originate from quantum states *connecting* the two wells *under* the barrier. Here, we present a mechanism that is based only upon the complex plane mechanics discussed above and avoids any additional *ad hoc* insertion of "barrier paths". Since the complex plane dynamics behaves as the usual classical real time mechanics, paths with $E < 0$ never cross the barrier. However, a full semiclassical treatment needs to account for the dominant fluctuations about the semiclassical paths. Now, for $T < T_c$ there is a whole family of loop-like orbits in the complex plane; all with the same energy, period, and action increase after one period differing from each other only by their respective phases, i.e. by their crossing points $q_f \le q_1$ with the real axis. It turns out that each time these orbits pass their end-coordinate q_f there are other trajectories of this family arbitrarily close in phase space (see fig. 4). The role of quantum mechanics then is to induce transitions between these orbits via small fluctuations. For sufficiently long times a path starting at a certain q_f near the barrier top may successively slip down to an orbit with another phase q_f', eventually reach the stable regions around $\pm q_a$, and fluctuate in the long time limit between these regions. That this scenario actually describes the low temperature coherent tunneling dynamics has been discussed briefly in [20] and will be described in some detail in the sequel.

For $T = 0$ the amplitude of the Euclidian time paths is $q_1 = q_a$. Thus, all stationary paths $q_s(q_f,t)$, $q_s'(q_f,t)$ have energy $E = V(q_a)$ and period $t_a \equiv t_p(q_a) = 2\pi/\omega_a$. Then, the Euclidian action $\bar{S}(q_i,q_i')$ suppresses energy fluctuations around $E = V(q_a)$ exponentially, so that classical paths running in time t from $q_i \neq q_s$ and $q_i' \neq q_s'$ to q_f and $-q_f$, respectively, i.e. with $E \neq V(q_a)$, are negligible. Further, studying the short action, $W(q,q') = \int_q^{q'} dq\,p \equiv S(q,q') + Et$,

one finds according to Eq. (43) that after each period $W(q_f, q_f) = W(q_a, q_a) = 0$. This result combined with the fluctuation prefactor [see Eq. (9)] gives for the Gaussian propagator after multiple round trips and for coordinates $q_f < q_a$

$$|G_{nt_a}(q_f, q_f)|^2 \propto \frac{1}{nt_a(q_a^2 - q_f^2)}, \quad n = 1, 2, 3, \ldots. \tag{51}$$

Hence, the probability to return to the starting point decreases as the number of periods increases. In contrast, in the vicinity of the wells the Gaussian propagator coincides with the harmonic propagator. To be more precise, due to caustics in the semiclassics of this simple propagator at all $nt_a/2$, an extended semiclassical analysis must be invoked leading to an Airy function; details of the procedure are well-known [27] and of no interest here. The important point is that in the barrier region the simple semiclassical return probability decays to zero for large times while in the well regions it remains constant. Thus, we conclude that the dominant quantum fluctuations neglected in the Gaussian approximation to the real time propagators are those that connect stationary paths with the same energy but different phases, i.e. initial coordinates q_f. Effectively, these relevant fluctuations shift q slightly away from the classical path $q_s(q_f, t)$ to reach another stationary path $q_s(q_f', t)$ (cf. fig 3). The corresponding change in action after a period and for small deviations is simply

$$W(q_f', q_f) \approx p_s(q_f, 0)(q_f' - q_f). \tag{52}$$

This repeats at subsequent oscillations. Hence, a "fluctuation path" can be characterized by its sequence of crossing points with the real axis after each round trip, e.g. by $q^{(k)}, k = 1, \ldots, n$ for $t = nt_a$ where $q^{(1)} = q_f$. Accordingly, a fluctuation path is not a classical path, i.e. it does not fulfill Newton's equation of motion, but can be seen as almost classical since it stays always in the close vicinity of a classical path. In the sequel we first explain the general structure of the extended semiclassical approximation and later on turn to details of the calculation.

As an example let us consider a fluctuation path starting at q_f that spirals around q_a while the crossing point $q^{(n)}$ with the real axis diffuses close to q_a and returns to q_f in $t \gg t_a$ (see fig. 5a). According to (52) on the way to q_a a particular path gathers an additional action $W^+(q_a, q_f)$ which is imaginary due to imaginary $p_s(q, 0)$ [see Eq. (12)] where

$$|W^+(q_a, q_f)| = \int_{q_f}^{q_a} dq \, \{2M[V(q) - V(q_a)]\}^{1/2} \tag{53}$$

and the $+$ $[-]$ sign stands for clockwise [anti-clockwise] rotation of the path in the complex plane. As long as the crossing point q_f does not diffuse the imaginary time path connecting the endpoints of the two real time paths coincides at $t = nt_a$ with the imaginary time orbit connecting $-q_f$ with q_f at $t = 0$. Taking into account the phase fluctuations, however, forces the endpoint of the imaginary time path to move with the endpoint $q^{(n)}$ of the "real time path" also towards q_a. The mapped imaginary time path after $t \gg t_a$ therefore runs from $-q_f$ to q_a. According to (12) the additional amount of Euclidian action required for this deformation of the imaginary time path exactly counterbalances $W(q_a, q_f)$ so that the total action Σ remains constant which reflects the stationarity of Σ along stationary paths. From close to q_a the fluctuation path spirals back to q_f. However, since q_a is a branching point of the momentum there are two channels: the real time fluctuation path can maintain the direction of rotation or pass the turning point (TP) q_a, thus changing the sense of rotation (cf. fig. 5a). In the former case on the way back from q_a to q_f the fluctuation path crosses the real axis with the same direction of momentum as on the way to q_a, so that due to $W^+(q, q') = -W^+(q', q)$ the path looses the action $W^+(q_a, q_f)$ again and returns to q_f with $W(q_f, q_f) = 0$. In the latter case, momenta on the way back have opposite direction to those on the way forth so that the path arrives at q_f with action $W(q_f, q_f) = W^+(q_a, q_f) + W^-(q_f, q_a) = 2W^+(q_a, q_f)$ and momentum $-p_s(q_f, 0)$.

Moreover, a fluctuation path starting at $q_f > 0$ can either move along the real axis to the right to reach q_a or move to the left to arrive at $-q_a$. In the latter case, the crossing point $q^{(n)}$ diffuses across the barrier top so that the path initially spiraling around q_a finally orbits around $-q_a$ with opposite sense of rotation. Accordingly, due to $W^+(q_a, 0) = -W^-(-q_a, 0)$ the real time action factor $\exp[iW(\pm q_a, 0)/\hbar]$ grows or decreases exponentially for diffusion to the right or to the left, respectively. In any case, near $\pm q_a$ the semiclassical propagator has to match onto the propagators in the harmonic wells. For the two lowest lying eigenstates which are relevant here, the matching procedure was discussed in detail by Coleman [28]. Correspondingly, these two states determine the relevant propagator in its spectral representation. Then, it turns out that a TP may only occur if $iW(q_f, \pm q_a) < 0$. This has profound consequences on the extended semiclassical approximation: (i) A relevant fluctuation path from q_f to q_f must reach $\pm q_a$ rotating clockwise to have a TP. Then $W^+(q_a, q_f) + W^-(q_f, q_a) = 2i|W(q_a, q_f)|$ and the corresponding

contribution to the propagator has an exponentially small factor $\exp[-2|W(q_a,q_f)|]$. (ii) A fluctuation path with more than one TP has to alternatively visit TPs at $\pm q_a$ thereby changing its sense of rotation repeatedly. In passing from one TP to the next the path gathers the action $W^-(0,-q_a)+W^+(q_a,0) = W^-(0,q_a)+W^+(-q_a,0) = i|W(q_a,-q_a)| \equiv i\bar{W}_a$ which coincides with the instanton action in Δ introduced in Eq. (41). Hence, according to (i) contributions from fluctuation paths with TPs do not play any role for short times. For longer times, however, they become increasingly important, particularly, since a fluctuation path may spend an arbitrary period of time at the TPs $\pm q_a$ where $V'(q_a)=0$ before leaving them. The detailed analysis shows (see below) that for $t \gg t_a$ the phase space of equivalent fluctuations with one TP is therefore $\propto t$ which compensates for the exponentially small action factor. Moreover, at each TP a path gathers an additional Maslov index $\nu \to \nu+1$. Then, according to (ii) the full density matrix is given by a sum over ν,ν' taking into account the proper order of TPs, i.e.

$$\rho(q_f,-q_f,t) = \sum_{\nu,\nu'\geq 0} \rho_{\nu,\nu'}(q_f,-q_f,t), \tag{54}$$

where $\rho_{\nu,\nu'}$ denotes the contribution from relevant fluctuation paths with ν TPs in the forward and ν' TPs in the backward propagator. Note that ν,ν' only label the TPs of the two real time paths. For each ν,ν' one has also to sum over all imaginary time paths connecting the endpoints of the real time orbits.

To evaluate the sum in Eq. (54) we start by analyzing the term with $\nu=\nu'=0$. As discussed above the diffusion of the real time orbits is then irrelevant and the imaginary time path has to run form $-q_f$ to q_f. To lowest order in Δ [see Eq. (40)] we have the two imaginary time paths $\bar{q}_\pm(q_f,\sigma)$ emerging at T_c that connect $-q_f$ with q_f via TPs at $\pm q_a$, respectively. At $T=0$ other solutions of the imaginary time dynamics with $r>1$ [cf. Eq. (36)] just contain additional intermediate instantons, i.e. imaginary time trajectories connecting q_a with $-q_a$ or vice versa. For an equilibrium initial preparation (small) fluctuations about the stationary paths towards $\pm q_a$, respectively, give identical contributions and we thus recover $\rho_\beta(q_f,-q_f)/Z$ [Eq. (40)] in the limit $T\to 0$ with the partition function

$$Z = 2\exp[-\beta V(q_a) - \beta\hbar\omega_a/2]\,\cosh(\hbar\beta\Delta/2). \tag{55}$$

For the nonequilibrium preparation, however, only fluctuations towards $-q_a$ contribute (fig. 5b). This way, one obtains for coordinates q_f near the barrier top

$$\begin{aligned}\rho_{0,0}(q_f,-q_f,t) &= \frac{1}{2}\lim_{\beta\to\infty}\frac{1}{Z}\rho_\beta(q_f,-q_f)\\ &= \frac{4}{\sqrt{2\pi}\delta_a}\,\exp[-\bar{W}_a/\hbar]\,\cosh\left(q_f q_a/4\delta_a^2\right)^2 \equiv \frac{1}{2}\,\psi_0(q_f)^2\end{aligned} \tag{56}$$

where we used the short action of an instanton $\bar{W}_a = \bar{W}(q_a,-q_a)$ with $\bar{W}_a = |W(q_a,-q_a)|$ and $\psi_0(q_f)$ denotes the semiclassical ground state wave function in the double well.

The next order real time paths are those with one TP, i.e. $\nu=1,\nu'=0$ and $\nu=0,\nu'=1$ in Eq. (54). Thereby, the real time path $q_s(t)$ makes an excursion from q_f via a TP at q_a to $-q_a$ in case where at $t=0$ the endpoints $-q_f$ and q_f are connected by an imaginary time path $\bar{q}_-$, while it diffuses from q_f via a TP at $-q_a$ to q_a in case of $\bar{q}_+$. Accordingly, one observes that for an equilibrium initial preparation all contributions cancel, e.g. the contribution corresponding to $\bar{q}_-$ with $\nu=1,\nu'=0$ cancels that corresponding to $\bar{q}_+$ with $\nu=0,\nu'=1$. In fact, it can be shown in the same way that for an equilibrium initial state *all* terms in the sum (54) with $\nu,\nu'>0$ vanish. However, for the initial preparation (3) a finite result follows due to the projection onto the left side of the complex plane. Hence, both real time orbits have to end near $-q_a$ whereby one trajectory has a TP at q_a. According to the above discussion we gain the following action factors: For $\nu=1,\nu'=0$ one has $\exp[-3|W(q_a,0)|/\hbar + q_a q_f/(4\delta_a^2)]$ from the forward and $\exp[-|W(q_a,0)|/\hbar + q_a q_f/(4\delta_a^2)]$ from the backward propagator (cf. fig. 5c) while $\nu=0,\nu'=1$ gives $\exp[-|W(q_a,0)|/\hbar - q_a q_f/(4\delta_a^2)]$ and $\exp[-3|W(q_a,0)|/\hbar - q_a q_f/(4\delta_a^2)]$ (cf. fig. 5d), respectively. After expanding the integrand in (1) around $-q_a$ up to second order, the ordinary integrations over the initial coordiates are seen to be restricted to the harmonic range around $-q_a$ so that the θ functions can be put to 1. Then, the integrals effectively describe the stationary real time motion of the equilibrium well distribution $\rho_\beta(-q_a,-q_a)$. Combining these findings yields

$$\begin{aligned}\rho_1(q_f,-q_f,t) &\equiv \rho_{1,0}(q_f,-q_f,t) + \rho_{0,1}(q_f,-q_f,t)\\ &= i8\,\Phi(t)\,\exp[-2|W(q_a,-q_a)|/\hbar]\,\sinh(q_f q_a/2\delta_a^2)\,\rho_\beta(-q_a,-q_a)/Z.\end{aligned} \tag{57}$$

Here $\rho_\beta(-q_a,-q_a)$ includes a sum over multi-instanton contributions of the imaginary time paths, resulting for $T\to 0$ in $\rho_\beta(-q_a,-q_a)/Z = \sqrt{M\omega_a/4\pi\hbar}$. Further, $\Phi(t)\propto t$ takes into account the phase space contribution from equivalent

fluctuation paths connecting q_f via a TP at q_a with $-q_a$. These paths differ only in their "sojourn times" at the TP q_a. To evaluate Φ we adopt the method outlined in [29] to which we also refer for further details and write

$$G_t(q_a,-q_a)=\int_0^t du\, G_{t-u}(q_a,0)\,\dot q_s(0,u)\,G_u(0,-q_a). \tag{58}$$

Since for $t\gg t_a$ the sojourn time is exponentially large, one can actually sum the intermediate time step u over the entire time interval up to negligible corrections. To calculate the semiclassical propagators in the integrand of (58) one exploits that a fluctuation path moving from $q=0$ to q_a in time $t\gg t_a$ spends almost all time by orbiting in the vicinity of q_a thereby diffusing along the classical stationary paths (42) with $q_f\lesssim q_a$ towards the TP. Hence, the time dependence of the propagators is determined only by the asymptotic behavior of the fluctuation paths. Then, as already derived in the previous paragraph, the actions turn out to be independent of time up to exponentially small corrections and their sum gives rise to the action factor $\exp[-|W(q_a,-q_a)|/\hbar]$ in $G_t(q_a,-q_a)$. For the prefactors one uses the representation (9), and exploits the fact that $\dot q_s(0,u)\sqrt{A_{t-u}(q_a,0)A_u(0,-q_a)}$ depends for $t\gg t_a$ on time and temperature only through $\exp[-(\hbar\beta+it)\omega_a/2]$ while its dependence on the intermediate time step u is exponentially small. This way, since both exponential factors are already accounted for in (57), we arrive at

$$\Phi(t)=G_t(q_a,-q_a)\exp[|W(q_a,-q_a)|/\hbar+(\hbar\beta+it)\omega_a/2] \tag{59}$$

which leads to

$$\Phi(t)=t\,\frac{4\omega_a q_a}{\sqrt{2\pi}\delta_a}. \tag{60}$$

Combining this result with Eq. (57) we derive the one-TP contribution to Eq. (54) as

$$\rho_1(q_f,-q_f,t)=it\Delta^2\,\sinh(q_aq_f/2\delta_a^2)/(\omega_aq_a) \tag{61}$$

where the tunnel splitting is specified in (41). Likewise, contributions from real time path with more than one TP can be calculated where the proper order of TPs must be taken into account. Eventually, only contributions with $i^{2k-1}\Delta^{2k}, k=1,2,\ldots$ survive and the time dependent density matrix (54) for coordinates near barrier top reads

$$\rho(q_f,-q_f,t)=\frac{1}{2}\psi_0(q_f,-q_f)^2+i\Delta\,\sin(\Delta t)\,\sinh(q_aq_f/2\delta_a^2)/(\omega_aq_a). \tag{62}$$

Hence, the initial state (3) develops an imaginary, time dependent part from which the tunneling current (5) is gained as

$$J(t)=\Delta\sin(\Delta t) \tag{63}$$

describing coherent tunneling between the wells. This shows that a systematic semiclassical analysis of the real time dynamics of the system covers also low temperature tunneling. We note that the tunnel splitting coincides exactly with the result of the instanton approach [see Eq. (41)] where Δ is related to the action of an *imaginary* time path. Within the real time description the "instanton dynamics" is replaced by the above-mentioned diffusion along the real axis in the complex coordinate plane.

Before we conclude this section let us briefly sketch how the crossover from coherent decay to incoherent tunneling occurs within the present formalism as the temperature is raised; details of the calculation will be presented elsewhere. For finite temperatures $T>0$ the energy of the stationary paths is $|\bar E_1|=|V(q_1)|<|V(q_a)|$ so that the TPs of the fluctuation paths $q_1<q_a$ are shifted towards the barrier top. Accordingly, $V'(q_1)\neq 0$ and the corresponding actions in Eq. (58) are no longer independent of time. Thus, the time interval $t\gg t_a$ may eventually exceed the region where the integrand gives a contribution so that $\Phi(t)\to\Phi_{\rm fl}$ saturates. We note that for a system with dissipation basically the same mechanism, namely, an effective action depending on time via damping induced correlations, may cause incoherent tunneling even at $T=0$.

V. ECKART BARRIER

As another instructive example we analyze in the following the transport across a genuine scattering potential, namely, the so-called Eckart barrier

$$V(q) = \frac{V_0}{\cosh(q/L_0)^2}. \tag{64}$$

Here, V_0 is the barrier height and L_0 the typical interaction range. We drop the condition $V(q=0)=0$ in this section so that energies are shifted by V_0. In fact, the real time dynamics in this potential is much simpler as in the double well: particles steadily injected from a thermal reservoir to the left of the barrier built up a flux across the barrier that is stationary for all times after a certain transient time has elapsed. Thus, the corresponding quantum dynamics is described by a barrier transmission rate for all temperatures. In a semiclassical expansion we use $\hbar/\sqrt{2ML_0^2V_0}$ as the small parameter which demands high and broad barriers.

A. Thermal equilibrium and stationary phase points

The solution of Newton's equation of motion for the Eckart barrier in imaginary time reads [30]

$$\bar{q}_0(q_f,\sigma) = L_0 \,\mathrm{arsinh}\left\{\sqrt{\frac{V_0-\bar{E}}{\bar{E}}}\sin\left[\omega(\bar{E})\sigma-\phi_f\right]\right\} \tag{65}$$

where we introduced the energy dependent frequency

$$\omega(\bar{E}) = \omega_b\sqrt{\frac{\bar{E}}{V_0}} \tag{66}$$

with the barrier frequency $\omega_b = \sqrt{2V_0/ML_0^2}$. Energy $\bar{E}$ and phase ϕ_f are determined by the boundary conditions $\bar{q}_0(q_f,0) = -q_f$ and $\bar{q}_0(q_f,\hbar\beta) = q_f$. Accordingly, employing one of these conditions to fix ϕ_f, the energy can be evaluated from

$$\omega(\bar{E})\hbar\beta = r\pi + [1+(-1)^r]\phi_f, \tag{67}$$

where for given temperature real solutions exist only for a finite number of integers $r \geq 0$. Accordingly, this nonlinear equation gives the amplitude of the semiclassical path. As a function of temperature the solutions (65) and (67) resemble those in the inverted double well potential (cf. Sec. IV A). Particularly, for $T < T_c$ again all paths with $r = 1$ have the same energy independent of q_f

$$\bar{E}_1 \equiv V(q_1) = \frac{\pi^2 V_0}{\omega_b^2\hbar^2\beta^2} \tag{68}$$

with amplitudes $\pm q_1$ and the same frequency $\omega_1 = \omega(\bar{E}_1)$. An important difference to the double well case, however, is that the amplitude q_1 of the paths here grows without any limit as $T \to 0$, i.e. $\bar{E}_1 \to 0$. Hence, the equilibrium density matrices $\rho_\beta(q_f,-q_f)$ differ qualitatively in the deep tunneling regime. While for the double well potential near $T=0$ contributions from all multi-instanton paths must be summed up [see Eq. (40)], here, the density matrix is dominated by the oscillating paths newly emerging around $T_c = \omega_b\hbar/k_\mathrm{B}\pi$ for *all* $T < T_c$. For further details of the Euclidian semiclassics we refer to [30].

Now, for the stationary phase points we obtain

$$q_s(t) = L_0 \,\mathrm{arsinh}\left\{\sqrt{\frac{V_0-\bar{E}}{\bar{E}}}\sin\left[\phi_f - i\omega(\bar{E})t\right]\right\}, \quad q_s'(t) = -q_s[(-1)^{r+1}t] \tag{69}$$

which are connected by the Euclidian path $\bar{q}_s(\sigma) = \bar{q}_0[\sigma + i(-1)^{r+1}t]$. Starting at q_f $[-q_f]$ the path $q_s(t)$ $[q_s'(t)]$ describes for large times an almost free motion parallel to the real axis in accordance with the asymptotically vanishing interaction $V(q) \to 0$ as $q \to \pm\infty$. The energy of $q_s(t)$ is controlled by temperature where qualitatively the two ranges $T > T_c$ and $T \leq T_c$ must be distinguished. In the first case, $\bar{E}$ depends on q_f and for $q_f > 0$ we find asymptotically, i.e. for $\omega(\bar{E})t \gg 1$,

$$q_s(q_f,t) \approx L_0 \,\mathrm{arsinh}\left[\frac{\sinh(q_f/L_0)}{2\sin(\omega_b\hbar\beta/2)}\mathrm{e}^{\omega(\bar{E})t}\right] - iL_0\left(\frac{\pi}{2} - \frac{\omega_b\hbar\beta}{2}\right) \tag{70}$$

so that for $T > T_c$ all stationary paths are restricted to the strip $i(L_0/2)[-(\pi - \omega_b\hbar\beta), (\pi - \omega_b\hbar\beta)]$ (cf. fig. 6). In the range $T < T_c$ and for end-coordinates $q_f < q_1$ the oscillating Euclidian paths determine the energy independent of q_f as $E = \bar{E}_1$ [see Eq. (68)] with the frequency $\omega_1 = \omega(\bar{E}_1)$. Hence, in $T \ll T_c$ *all* path starting in the barrier range ($q_f \lesssim L_0$) nearly coincide asymptotically (see also fig. 6) for $\omega_b t \gg 1$

$$q_s(q_f, t) \approx q_1 + L_0 \ln[\sinh(\omega_1 t)] + iL_0\pi/2. \tag{71}$$

Orbits with $q_f > L_0$ come also close to $iL_0\pi/2$ but on a larger time scale, e.g. for q_f close to $q_1 \gg L_0$ on the scale $1/\omega_1$. Since $\mathrm{Im}\{q_s'\} \to -iL_0\pi/2$ for large t we conclude that the real time stationary phase dynamics for $T < T_c$ is restricted to the strip $[-iL_0\pi/2, iL_0\pi/2]$ in the complex plane (fig. 6). To complete this discussion we address the special cases $q_f = q_1$ and $q_f = 0$, respectively. In the former case the motion starts with zero momentum and takes place along the real axis, asymptotically ($\omega_1 t \gg 1$) as

$$q_s(t, q_1) \approx q_1 + L_0\omega_1 t. \tag{72}$$

In the latter case the orbit can only be defined as the limiting trajectory of $q_s(t, q_f)$ for $q_f \to 0$, thus, running along the imaginary axis from $q = 0$ to $q = iL_0\pi/2$ and afterwards parallel to the real axis.

The described complex plane dynamics depends essentially on the analytic properties of the potential $V(q)$. Interestingly, in case of the Eckart barrier one has for complex q the periodicity

$$V(q) = V(q + iL_0 n\pi), \quad n \text{ integer}. \tag{73}$$

Hence, the complex plane falls into strips $[(2n-1)iL_0\pi/2, (2n+1)iL_0\pi/2], n$ integer, parallel to the real axis each of which with identical classical mechanics and corresponding stationary phase paths $q_s(q_f + iL_0 n\pi, t)$. As shown above, for $T < T_c$ the real time dynamics starting from the real axis at $t = 0$ reaches asymptotically the boundaries of the strip $n = 0$, while in the range $T > T_c$ it does not. This has crucial impact on the semiclassical analysis for low temperatures as will be discussed in Sec. V C.

B. Stationary flux for high and moderate low temperatures

The systems starts from an initial state where the thermal equilibrium is restricted to the left of the barrier, thus extending to $q \to -\infty$. Accordingly, after a certain transient time has elapsed the flux across the barrier remains stationary forever. Since with increasing time the stationary phase points move away from the barrier top, for large times fluctuations of the order of L_0 or larger are needed to shift q_i into the region $\mathrm{Re}\{q_i\} \leq 0$, then rendering the Gaussian stationary phase approximation insufficient. Yet, we can use Eq. (17) to gain J_{fl} as long as the flux becomes stationary on a time scale within which q_s remains smaller than L_0.

In the range $T > T_c$ and for q_f near the barrier top one has $\bar{E} \approx V_0$ so that $\omega(\bar{E}) \approx \omega_b$. Then, the density matrix $\rho(q_f, -q_f, t)$ tends to stationarity on the scale $1/\omega_b$ while $q_s(t)$ reaches L_0 on the much longer time scale $\ln[V_0/(\bar{E} - V_0)]$ only. We thus regain within this time window approximatively the parabolic result (29) in the semiclassical limit – large V_0 and L_0 – where anharmonicities are negligibly small. Correspondingly, the rate reads as specified in Eq. (31) with $\omega_b = \sqrt{2V_0/ML_0^2}$.

For temperatures $T < T_c$ the transient time range grows according to $1/\omega_1 = \hbar\beta/\pi$, while the upper bound for the validity of the Gaussian approximation eventually shrinks to $1/\omega_b$. Hence, while one can no longer use the local barrier dynamics for temperatures $T \ll T_c$, in a region sufficiently close to T_c a rate calculation along the lines described in Sec. IV C still makes sense. Accordingly, for $T \lesssim T_c$ the density matrix is obtained as in Eq. (46) with the amplitude q_1 derived from Eq. (67) for $r = 1$ as

$$q_1 = L_0 \,\mathrm{arsinh}\left[\frac{\sqrt{(\omega_b\hbar\beta)^2 - \pi^2}}{\pi}\right]. \tag{74}$$

This way, one gets the rate

$$\Gamma = \frac{\omega_b}{4\pi^2 Z} \, \frac{\sqrt{(\omega_b\hbar\beta)^2 - \pi^2}}{\mathrm{arsinh}\left[\sqrt{(\omega_b\hbar\beta/\pi)^2 - 1}\right]} \, \exp\left(-\beta V_0\right) \tag{75}$$

for temperatures below T_c but still above $T_c/2$. For even lower temperatures higher order terms in the expansion around the stationary phase points q_s, q_s' must be taken into account. In the following section we show that for T

below $T_c/2$ the rate is dominated by quantum tunneling which requires an extended semiclassical analysis. Thus, a higher order expansion is needed only in the close vicinity of $T_c/2$ where the changeover from the thermal to the quantum rate occurs.

C. Stationary flux for low temperatures

The breakdown of the Gaussian stationary phase approximation for lower temperatures indicates also a breakdown of the simple semiclassical approximation to the real time propagators for large times. In fact, one needs to carefully analyze the quantum fluctuations around the classical paths to capture tunneling processes. In the sequel we proceed in the spirit of Sec. IV D and search for relevant phase fluctuations.

We begin by recalling that in the range $T \ll T_c$ and for coordinates $q_f < q_1$ the classical mechanics in the complex plane takes place in strips $[(2n-1)iL_0\pi/2, (2n+1)iL_0\pi/2], n$ integer, parallel to the real axis. One thus has families of classical paths (cf. fig. 6) all with the same energy $\bar{E}_1$ that start at $t \to -\infty$ to the far right on the lines $(2n-1)iL_0\pi/2$, run close together with almost vanishing momentum $-ML_0\omega_1$ towards the barrier top, pass at $t = 0$ the coordinates $q_f + inL_0\pi$ and then leave again to the far right moving close together with momentum $ML_0\omega_1$ asymptotically along the lines $(2n + 1)iL_0\pi/2$. Accordingly, for $T \to 0$ in classical phase space, see fig. 7, orbits with different phases ϕ_f, i.e. different q_f, but from the same or from adjacent strips lie arbitrarily close to each other in the asymptotic range where $|V(q)| \to 0$. The effort of quantum fluctuations then is to link these paths which reflects the asymptotically free particle diffusion in the Eckart potential. In simple semiclassical approximation one has asymptotically the propagator

$$G_t(q, q') = \left(\frac{M}{2\pi i\hbar t}\right)^{1/2} \exp\left[iM\frac{(q-q')^2}{2\hbar t}\right] \tag{76}$$

so that for fixed $q - q'$ and large times the transition probability decreases as $|G_t(q, q')|^2 \propto 1/t$ [cf. Eq. (51)]. Correspondingly, two different types of fluctuations can be identified: one type of fluctuations connects paths $q_s(q_f + iL_0n\pi, t)$ and $q_s(q'_f + iL_0n\pi, t)$ within the same strip, while the other type of fluctuations switches between paths $q_s(q_f + iL_0n\pi, t)$ and $q_s(q'_f + iL_0(n + 1)\pi, t)$ in adjacent strips. The first type is already accounted for in the simple semiclassical approximation to the real time propagator since these fluctuations never leave strip $n = 0$ and stay in the close vicinity to the asymptotic $q_s(q_f, t)$. In contrast, the second type is relevant beyond the Gaussian semiclassics since it causes large deviations and allows a path $q_s(q_f, t)$ by subsequently diffusing to another strip to reach a path $q_s(q'_f + iL_0n\pi, t)$ with q'_f far from q_f and n large. Interestingly, this second kind of fluctuations does not exist for $T > T_c$ where asymptotically there is always a gap $i\omega_b\hbar\beta$ between paths in adjacent strips (see fig. 6).

As an example let us consider a trajectory $q_s(q_f, t)$ with q_f close to the barrier top for $T \ll T_c$ and times $t \gg 1/\omega_1 \gg 1/\omega_b$. In this limit the orbit runs for $\omega_b t \gg 1$ along the boundary $iL_0\pi/2$ of the strip $n = 0$ where fluctuations of the second class bridge the tiny gap to an orbit $q_s(q'_f + iL_0\pi, t)$ with a different q'_f in the strip $n = 1$. This trajectory passes $q'_f + iL_0\pi$, and exploiting the periodicity of $V(q)$ the corresponding change in action $W(q_f, q'_f)$ is shown to read as in Eq. (52). Obviously, the described fluctuations always lead from an outgoing to an ingoing orbit thereby increasing the strip number which in turn requires a momentum fluctuation of order $2|\dot{q}_s(t)| = 2ML_0\omega_1$. Estimating typical momentum fluctuations by $\hbar/L_0$ one rederives from $\hbar/L_0 \gg ML_0\omega_1$ the condition $T \ll T_c$ so that at low temperatures these fluctuations will indeed occur. By the same procedure the path $q_s(q'_f + iL_0\pi, t)$ can be linked to a path $q_s(q''_f + iL_02\pi, t)$ and so forth. Similar as in case of the double well potential a "fluctuation path" is characterized by its sequence of crossing points $q^{(k)} + iL_0k\pi$, $k = 0, 1, 2, \ldots, n$ $[q^{(0)} = q_f]$, with the lines $iL_0k\pi$, i.e. the copies of the real axis in the strips k. Accordingly, for very large times $t \gg 1/\omega_1$ the point $q^{(n)} + iL_0n\pi$ moves with increasing n along the positive imaginary axis while simultaneously $q^{(n)}$ can slide down the real axis and away from the barrier top to reach the proximity of q_1. From close to q_1 relevant fluctuation paths traverse q_1 as a turning point (TP) – q_1 is a branch point for the momentum – and return via the described scenario to q_f in the strip $k = 0$, however, crossing the lines $iL_0k\pi$ with opposite direction of momentum as on the way forth. The total change in action is imaginary and given by $W(q_f, q_f) = W(q_1, q_f) - W(q_f, q_1) = 2W(q_1, q_f)$, n arbitrary but large, where for q_f close to the top

$$\begin{aligned} |W(q_1, q_f)| &= \int_{q_f}^{q_1} dq\,[2M(V(q) - V(q_1))]^{1/2} \\ &= \frac{\pi V_0}{\omega_b}\left(1 - \frac{\pi}{\omega_b\hbar\beta}\right) - \omega_b ML_0q_f. \end{aligned} \tag{77}$$

In a similar way, the sequence of $q^{(n)}$ of a fluctuation path starting at q_f can move directly towards the barrier top, diffuse across the barrier to enter the left halfplane of the complex plane, and end up in the asymptotic region $\mathrm{Re}\{q\} \to$

$-\infty$. Since in leading order the semiclassical propagator has asymptotically to match onto the free propagator (76), a TP may only occur if $iW(q_f, \pm q_1) < 0$. Hence, what we discussed in Sec. IV D [see paragraph above Eq. (54)] can directly be transfered to the situation here and the density matrix can be cast into the same form as in Eq. (54). In a notable difference to the double well potential, however, the TP q_1 here is not an isolated extremum of the potential meaning that each TP – for Euclidian and real time fluctuation paths as well – is *not* related to an additional phase factor for equivalent paths.

After having elucidated the general structure of the semiclassical density matrix we now turn to the explicit calculation of the sum (54) and begin with the term $\rho_{0,0}(q_f, -q_f, t)$. This matrix element follows by the same arguments as given in Sec. IV D. Since the equilibrium density matrix for the Eckart barrier is dominated by the oscillating paths newly emerging around T_c for all lower temperatures, all further contributions from Euclidian trajectories with $r \neq 1$ in Eq. (67) are negligible. Accordingly, we find for coordinates around the barrier top

$$\begin{aligned}\rho_{0,0}(q_f, -q_f) &= \frac{1}{2} \lim_{T \ll T_c} \frac{1}{Z} \rho_\beta(q_f, -q_f) \\ &= \frac{1}{ZL_0} \left\{ \frac{\pi V_0}{\omega_b^2 \hbar^2 \beta [(\omega_b \hbar \beta)^2 (1 - q_f^2/L_0^2) - \pi^2]} \right\}^{1/2} \exp\left[-\frac{\pi V_0}{\omega_b \hbar} \left(2 - \frac{\pi}{\omega_b \hbar \beta} \right) \right]. \end{aligned} \tag{78}$$

Note that in contrast to bounded systems the above density matrix remains temperature dependent even for $T \ll T_c$.

To next order real time paths with $\nu = 1, \nu' = 0$ and $\nu = 0, \nu' = 1$, respectively, contribute (cf. figs. 5c,d). For $t \gg 1/\omega_1$ a relevant real time fluctuation path with $\nu = 1$ starting at q_f moves via a TP at $q_1 + iL_0 n' \pi$, n' large, to the left halfplane where it eventually crosses $-q_1 + iL_0 n\pi$, n large, to run along the line $iL_0 n\pi$ and reach $q_i + iL_0 n\pi$ in the far left. For the segment of the fluctuation path from q_f via a TP to $-q_1 + iL_0 n\pi$ the corresponding action factor is $\exp[-3|W(q_1, 0)|/\hbar + \omega_b M L_0 q_f/\hbar]$. Due to the periodicity (73) of the potential the segment from $-q_1 + iL_0 n\pi$ to $q_i + iL_0 n\pi$, $q_i < -q_1$, can just be treated as the corresponding one along the real axis; for very large times $\omega_1 t \gg 1$, i.e. $|q_i| \gg q_1$ according to Eq. (72), we then get the action factor $\exp[-iMq^2/2\hbar t]$. Hence, the corresponding relevant real time propagator reads

$$G_t(q_f, q_i) = -i\sqrt{A(q_f, q_i)} \exp\left[-\frac{3|W(q_1, 0)|}{\hbar} + \frac{\omega_b M L_0 q_f}{\hbar} + iM \frac{q_i^2}{2\hbar t} \right]. \tag{79}$$

Similar, the propagator from $-q_f$ directly to $q_i' + iL_0 n\pi$ is gained. The crucial point is now that for the integral in Eq. (1) there are no longer isolated stationary phase points but rather *all* q_i, q_i' on the line $iL_0 n\pi$ and to the far left of the barrier top make the integrand for very large times stationary. The ordinary integrals in Eq. (1) can thus be seen as sums over stationary phase points q_i, q_i' whereby their distance is weighted by the asymptotic thermal distribution, i.e. in leading order the free particle equilibrium density matrix

$$\rho_\beta(q, q') = \left(\frac{M}{2\pi\hbar^2 \beta} \right)^{1/2} \exp\left[-\frac{M(q - q')^2}{2\hbar^2 \beta} \right]. \tag{80}$$

Accordingly, for $T \to 0$ one has $\rho_\beta(q_i, q_i') \to \delta(q_i - q_i')$ so that contributions from $q_i \neq q_i'$ are caused by thermal fluctuations at elevated temperatures. Further, for large q_i, q_i' and large times the prefactors $A(q_f, q_i)$ and $A'(-q_f, q_i')$, respectively, are independent of q_i, q_i', thus allowing us to carry out the q_i, q_i' integrals over the exponentials only. Then, using $-q_1$ as an upper bound for the asymptotic coordinate range it turns out that for $\omega_1 t \gg 1$ the result for the integrals in leading order is $\pi\hbar t/M$. Now, combining all factors we finally obtain the time independent density

$$\begin{aligned}\rho_1(q_f, -q_f) &= \lim_{\omega_1 t \gg 1} \rho_{1,0}(q_f, -q_f, t) + \rho_{0,1}(q_f, -q_f, t) \\ &= \frac{i}{ZL_0} \left[\frac{4\pi V_0}{\hbar \omega_b (\omega_b \hbar \beta)^3} \right]^{1/2} \sinh(2\omega_b M L_0 q_f/\hbar)\, \mathrm{e}^{-4|W(q_1,0)|/\hbar} \end{aligned} \tag{81}$$

where $|W(q_1, 0)|$ follows from Eq. (77). Employing the same procedure, contributions in the sum (54) from real time paths with more than one TP can be derived, however, they contain additional action factors and are thus exponentially small compared to ρ_1. Hence, the stationary semiclassical density matrix for low temperatures and very large times is found as

$$\rho_{\mathrm{fl}}(q_f, -q_f) = \frac{1}{2Z} \rho_\beta(q_f, -q_f) + \rho_1(q_f, -q_f) \tag{82}$$

with ρ_β as specified in Eq. (78). Finally, from Eq. (5) we gain the thermal tunneling rate

$$\Gamma = \frac{1}{Z}\left[\frac{4\pi V_0 \omega_b}{\hbar(\omega_b\hbar\beta)^3}\right]^{1/2} \mathrm{e}^{-4|W(q_1,0)|/\hbar}. \tag{83}$$

This simple formula is applicable as long as $q_1 > L_0$, a temperature range which can be estimated by T below $T_c/2$, or equivalently $\omega_b\hbar\beta > 2\pi$. To be precise, there is also a lower bound for the temperature. Namely, for $T \to 0$ any semiclassics in the Eckart barrier breaks down due to the fact that then tunneling takes place in the low energy range near the base of the barrier where the wave length of a wave function tends to exceed the width of the barrier. From the known exact transition probability [see e.g. [30]] one derives that this scenario becomes relevant for $\omega_b\hbar\beta \gg 2\pi^4(V_0/\hbar\omega_b)$ corresponding in the semiclassical limit $V_0/\hbar\omega_b \gg 1$ to extremely low temperatures. In the broad temperature range between these bounds, i.e. $2\pi < \omega_b\hbar\beta \lesssim 2\pi^4(V_0/\hbar\omega_b)$, the above rate expression describes the decay rate with remarkable accuracy when compared to the exact result even for moderate barrier heights (see fig. 8). Table I presents a numerical comparison with results from other approaches. For temperatures above $T_c/2$ the real-time semiclassical rate is slightly too small and coincides for $T > T_c$ with the well-known "unified" semiclassical rate formula gained by the thermal average over the transmission $T(E) = 1/\{1 + \exp[S(E)/\hbar]\}$, where $S(E)$ is the bounce action for $T < T_c/2$. The small deviations from the exact rate are due to the fact that in the simple version of the theory presented here anharmonicities of the potential are neglected for $T > T_c$ and taken into account only in leading order in $T_c > T > T_c/2$. A perturbative expansion in an anharmonicity parameter allows for a systematic improvement. For the same reason, the temperature region around $T_c/2$ is not well described. In the deep tunneling region $T < T_c/2$, which is notoriously problematic for real-time rate theories, our theory performs excellently. In fact, the low temperature formula (83) turns out to be identical to the result derived within the instanton/bounce approach [see e.g. [31]]. The bounce is an oscillating Euclidian orbit, periodic in phase space, which connects $q_f = 0$ with itself, thus emerging as a solution of Eq. (67) at $T = T_c/2$ $(r = 2)$. While in imaginary time methods the bounce trajectory describes barrier penetration, here, effectively the same tunneling rate arises from *fluctuations around real time paths* the energy of which is fixed by oscillating Euclidian orbits, closed in phase space, emerging at T_c $(r = 1)$. These latter minimal action paths solely determine the semiclassical thermal equilibrium for lower temperatures $T < T_c$, thus establishing within a semiclassical real time approach the relation between the thermal density matrix and the thermal tunneling rate, since long an open question in thermal rate theory.

TABLE I. Transmission factor $P = \Gamma/\Gamma_{cl}$ for the symmetric Eckart barrier. Γ_{cl} is the classical rate and parameters are the same as in fig. 8.

$\omega_b\hbar\beta$	$P^{\mathrm{a}}_{\mathrm{rsemi}}$	$P^{\mathrm{b}}_{\mathrm{uni}}$	$P^{\mathrm{c}}_{\mathrm{QTST}}$	P^{d}_{SQTST}	P^{e}_{ex}
1.5	1.10	1.10	1.13	1.13	1.13
3	1.50	1.50	1.54	1.52	1.52
5	2.98	3.84	3.18	–	3.11
6	3.86	8.92	5.74	2.2	5.2
8	21.99	17.97	29.3	11.9	21.8
10	136.2	132.2	248	149	162
12	1613	1606	3058	3006	1970
16	$6.03 \cdot 10^5$	$6.03 \cdot 10^5$	–	$2.56 \cdot 10^6$	$7.41 \cdot 10^5$
18	$1.54 \cdot 10^7$	$1.54 \cdot 10^7$	–	$9.1 \cdot 10^7$	$1.88 \cdot 10^7$

[a] P_{rsemi} is the transmission factor as derived by the real-time semiclassical approach presented in this paper

[b] P_{uni} is the transmission factor of the "unified" semiclassical approach

[c] P_{QTST} is the transmission factor according to the simplest version of Pollak's QTST, from Ref. [32]

[d] P_{SQTST} is the transmission factor according to the full semiclassical version of Pollak's QTST, from Ref. [32]

[e] P_{ex} is the exact transmission factor

This represents substantial progress when compared with other attempts. While Pollak's new quantum transition state theory [11] is based on a numerically exact evaluation of the thermal flux, it suffers from a simple semiclassical approximation to the real time propagators. In the associated full semiclassical calculation by Pollak and Eckhardt [32] only half of the bounce action appears in the exponential factor for temperatures below $T_c/2$ and the corresponding tunneling rates are too large (see also Table I). The centroid method [10] gives the correct action factor, however, its semi-empirical factorization of thermal and dynamical contributions leads to a prefactor which is too small for lower temperatures. Finally, from semiclassical real time calculations for the Eckart barrier based on the simple semiclassical propagator [17,18] tunneling probabilities in the deep tunneling regime cannot be properly extracted since they depend strongly on the initial state.

VI. CONCLUSIONS

We have developed a unified semiclassical theory that describes the real time dynamics of quantum statistical systems for all temperatures including coherent and incoherent processes. Starting from the exact nonequilibrium dynamics the approximate density matrix is gained by employing semiclassical propagators in real and imaginary time combined with a stationary phase evaluation. Accordingly, the relevant classical mechanics takes place in the complex coordinate plane where the energy of classical real time trajectories is fixed by the Euclidian orbits determining the equilibrium distribution. Consequently, real time paths follow by solving an initial value rather than a boundary value problem. While this procedure can be used to study the dynamics for a wide class of systems and initial conditions, here, we concentrated on the flux across a double well potential and an Eckart barrier. Then, for high to moderate temperatures the Gaussian approximation suffices to obtain a stationary flux. In the tunneling domain, however, this approximation fails and the complex plane dynamics allows to identify the dominant quantum fluctuations in the real time propagators. These are zero-mode like phase fluctuations which give rise to a diffusion along the scaffold of classical orbits. Quantum tunneling in the real time domain can semiclassically thus be interpreted as a diffusion process on a certain family of classical real time paths. By systematically incorporating the phase fluctuations we managed to derive for the first time within a real time semiclassical formalism coherent tunneling dynamics.

Regarding incoherent decay in the deep tunneling regime, the theory revealed the connection between thermal equilibrium and the tunneling rate upon which thermodynamic rate formulas are based. In the semiclassical limit flux across the barrier and equilibrium are linked via the intimate relation between Euclidian and real time paths in the complex plane mechanics. However, the theory not only reproduces the results of various other semiclassical thermal rate theories for higher temperatures, but covers with no further assumptions also the low temperature regime where so far other real time methods failed.

Several questions could not be analyzed in detail in this article: There is first the temperature range around $T_c/2$ where approximately high and low temperature semiclassics match; we briefly sketched corresponding improvements. Second, we only touched in passing the explicit real time dynamics in the transient time domain where for incoherent processes the relaxation to a stationary flux occurs. Third, other initial preparations, e.g. to gain correlation functions, were out of the scope of this paper.

Moreover, with the appropriate formalism at hand further extentions are possible. While the dynamics of dissipative systems was already studied in the high to moderate temperature range [21,26], the low temperature tunneling regime is now in principle open for investigations. Of course, a crucial point for all further applications is to develop an appropriate numerical algorithm to mimic the "diffusion" in the complex plane. We hope to make progress in this direction in the near future.

ACKNOWLEDGMENTS

We thank P. Pechukas for many interesting discussions. JA acknowledges a Feodor Lynen fellowship of the Alexander von Humboldt Foundation. Further support was provided by the DAAD and the DFG through SFB276.

---

[1] P. Hänggi, P. Talkner, and M. Borkovec, Rev. Mod. Phys.**62**, 251 (1990) and references therein.

[2] J.S. Langer, Ann. Phys. (NY) **41**, 108 (1967).
[3] H. Grabert, P. Olschowski, and U. Weiss, Phys. Rev. B **36**, 1931 (1987).
[4] W. Miller, J. Chem. Phys. **62**, 1899 (1975).
[5] P. Hänggi and W. Hontscha, J. Chem. Phys. **88**, 4094 (1988); Ber. Bunsenges. Phys. Chem. **95**, 379 (1991).
[6] M.C. Gutzwiller, Physica D **5**, 183 (1982).
[7] G. A. Voth, D. Chandler, and W. H. Miller, *J. Chem. Phys.* **91**, 7749 (1989).
[8] T. Yamamoto, J. Chem. Phys. **33**, 281 (1960).
[9] W. H. Miller, S. D. Schwartz, and J. W. Tromp, J. Chem. Phys. **70**, 4889 (1983).
[10] G. A. Voth, D. Chandler, and W. H. Miller, *J. Phys. Chem.* **93**, 7009 (1989).
[11] E. Pollak, *J. Chem. Phys.* **107**, 64 (1997); E. Pollak and J.-L. Liao, *ibid.* **108**, 2733 (1998).
[12] J. Shao, J.-L. Liao, and E. Pollak, J. Chem. Phys. **108**, 9711 (1998).
[13] H. Wang, X. Sun and W. H. Miller, *J. Chem. Phys.* **108**, 9726 (1998); X. Sun, H. Wang and W. H. Miller, *ibid.* **109**, 4190 (1998).
[14] A.J. Leggett, S. Chakravarty, A.T. Dorsey, M.P.A. Fisher, A. Garg, and W. Zwerger, Rev. Mod. Phys. **59**, 1 (1987).
[15] U. Weiss, *Quantum Dissipative Systems*, (World Scientific, Singapore, 1993).
[16] H.A. Kramers, Physica **7**, 284 (1940).
[17] S. Keshavamurthy and W.H. Miller, Chem. Phys. Lett., **218**, 189 (1994).
[18] F. Grossmann and E.J. Heller, Chem. Phys. Lett. **241**, 45 (1995).
[19] N.T. Maitra and E.J. Heller, Phys. Rev. Lett., **78**, 3035 (1997).
[20] J. Ankerhold and H. Grabert, Europhys. Lett. **47**, 285 (1999).
[21] J. Ankerhold, H. Grabert, G.L. Ingold, Phys. Rev. E **51**, 4267 (1995); J. Ankerhold, H. Grabert, Chem. Phys. **204**, 27 (1996).
[22] W.H. Miller, Adv. Chem. Phys. **XXV**, 69 (1974).
[23] For the case of pure real time dynamics see: M.V. Berry and K.E. Mount, Rep. Prog. Phys. **35**, 315 (1972).
[24] J. Ankerhold and H. Grabert, Physica A **188**, 568 (1992).
[25] M. Abramowitz and J.E. Stegun (eds.), *Handbook of Mathematical Functions*, (National Bureau of Standards, 1972).
[26] J. Ankerhold and H. Grabert, Phys. Rev. E **52**, 4704 (1995); *ibid.* **55**, 1355 (1997).
[27] L.S. Schulman, *Techniques and Applications of Path Integrals*, (Wiley, New York, 1981).
[28] S. Coleman, in *The Whys of Subnuclear Physics*, A. Zichichi (ed.), (Plenum, New York, 1979).
[29] U. Weiss, W. Haeffner, Phys. Rev. D, **27**, 2916 (1983).
[30] F.J. Weiper, J. Ankerhold, and H. Grabert, J. Chem. Phys. **104**, 7526 (1996).
[31] J. Cao and G.A. Voth, J. Chem. Phys. **105**, 6856 (1996).
[32] E. Pollak and B. Eckhardt, *Phys. Rev. E* **58**, 5436 (1998).

FIG. 1. Loop of stationary imaginary and real time paths in the complex time plane $z = u + i\sigma$.

FIG. 2. Semilcassical paths (dashed lines) in the complex plane near the parabolic barrier top. Shaded area contains relevant intermediate coordinates q_i, q_i' reached by fluctuations along arrows.

FIG. 3. Real time paths in the double well potential with wells at $\pm q_a$ (dots) for various q_f and $T = 0$ (thin lines). The thick line shows a typical fluctuation connecting orbits with different q_f.

FIG. 4. Phase spaces orbits of complex real time paths in the double well potential at $T = 0$. In the left picture the real part of the orbits is shown for trajectories starting with $q_f > 0$ near the barrier top; the dot indicates the well at q_a. In the right picture the corresponding imaginary parts are depicted.

FIG. 5. Diffusion of the crossing point $q^{(n)}$ of a fluctuation path along the real axis (thick lines) for various cases discussed in the text. Dots indicate the wells at $\pm q_a$ that are branch points for the momenta, thin vertical lines the end-coordinates at $\pm q_f$. Solid lines refer to the forward, dotted ones to the backward propagator, a crossing of a dot a TP.

FIG. 6. Real time paths in the complex plane for the Eckart barrier. Solid lines show orbits for $T < T_c$, dotted lines orbits for $T > T_c$.

FIG. 7. Phase space orbits of complex real time paths in the Eckart barrier potential at $T \ll T_c$. In the left picture the real part of the orbits is shown for trajectories starting with $q_f > 0$ near the barrier top. In the right picture the corresponding imaginary parts are depicted; the dotted line separates the strips $n = 0$ and $n = 1$.

FIG. 8. Transmission factor P as a function of inverse temperature for an Eckart barrier with $\alpha = 12$, $\alpha = 2\pi V_0/\hbar\omega_b$. P is defined by $P = \Gamma/\Gamma_{cl}$ with Γ_{cl} the classical rate, i.e. the high temperature limit to Eq. (31). The solid line is the exact result. In the left picture the dotted line shows the parabolic result Eq. (31), the dashed line represents Eq. (75), and the arrow indicates the inverse temperature corresponding to T_c. In the right picture the dashed line depicts the result Eq. (83) and the arrow refers to $T_c/2$.

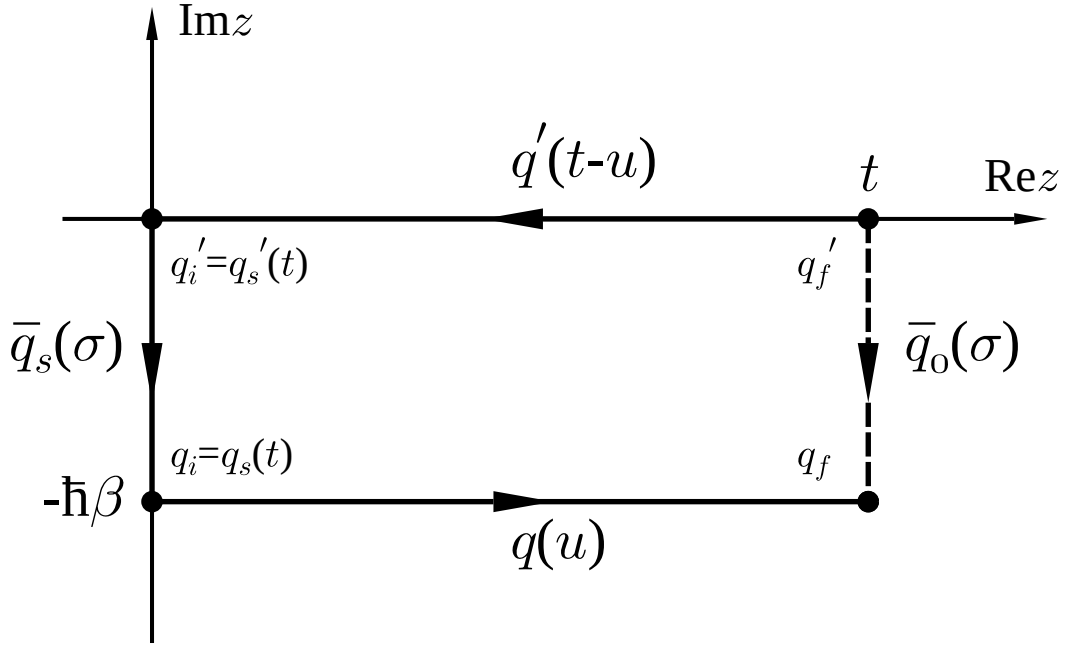

Figure 1, Ankerhold et al

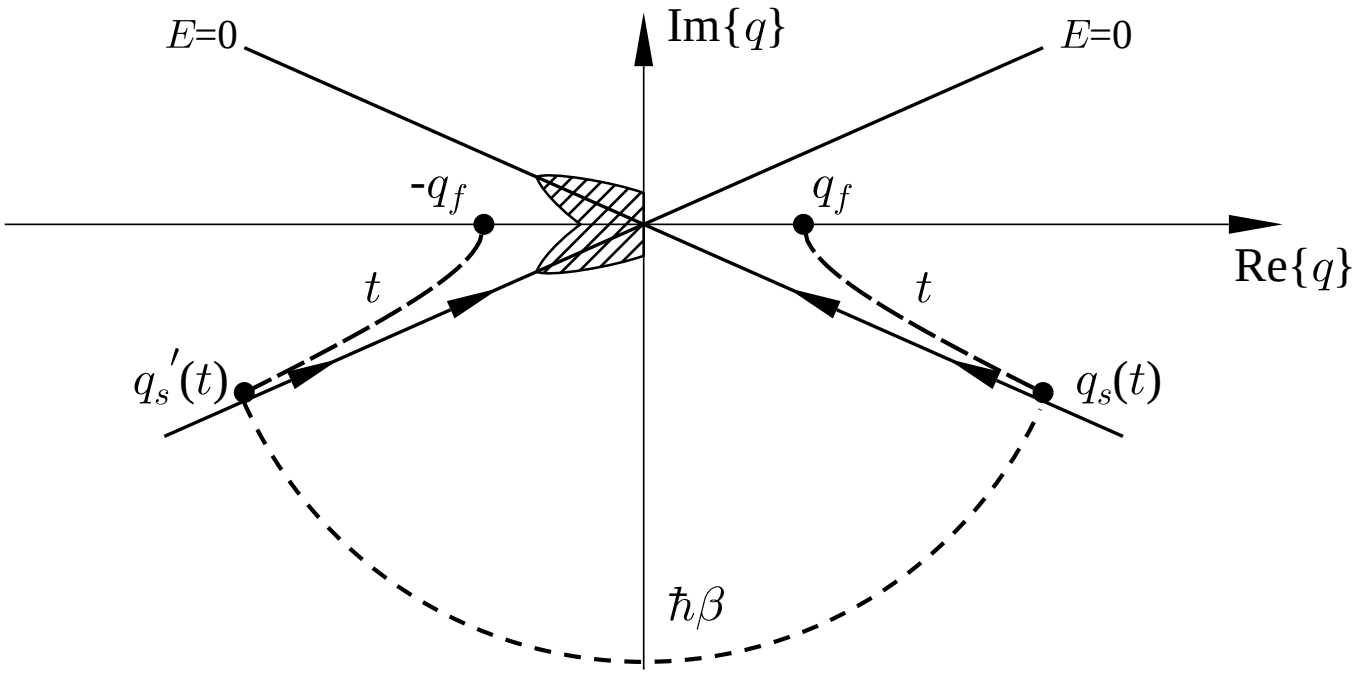

Figure 2, Ankerhold et al

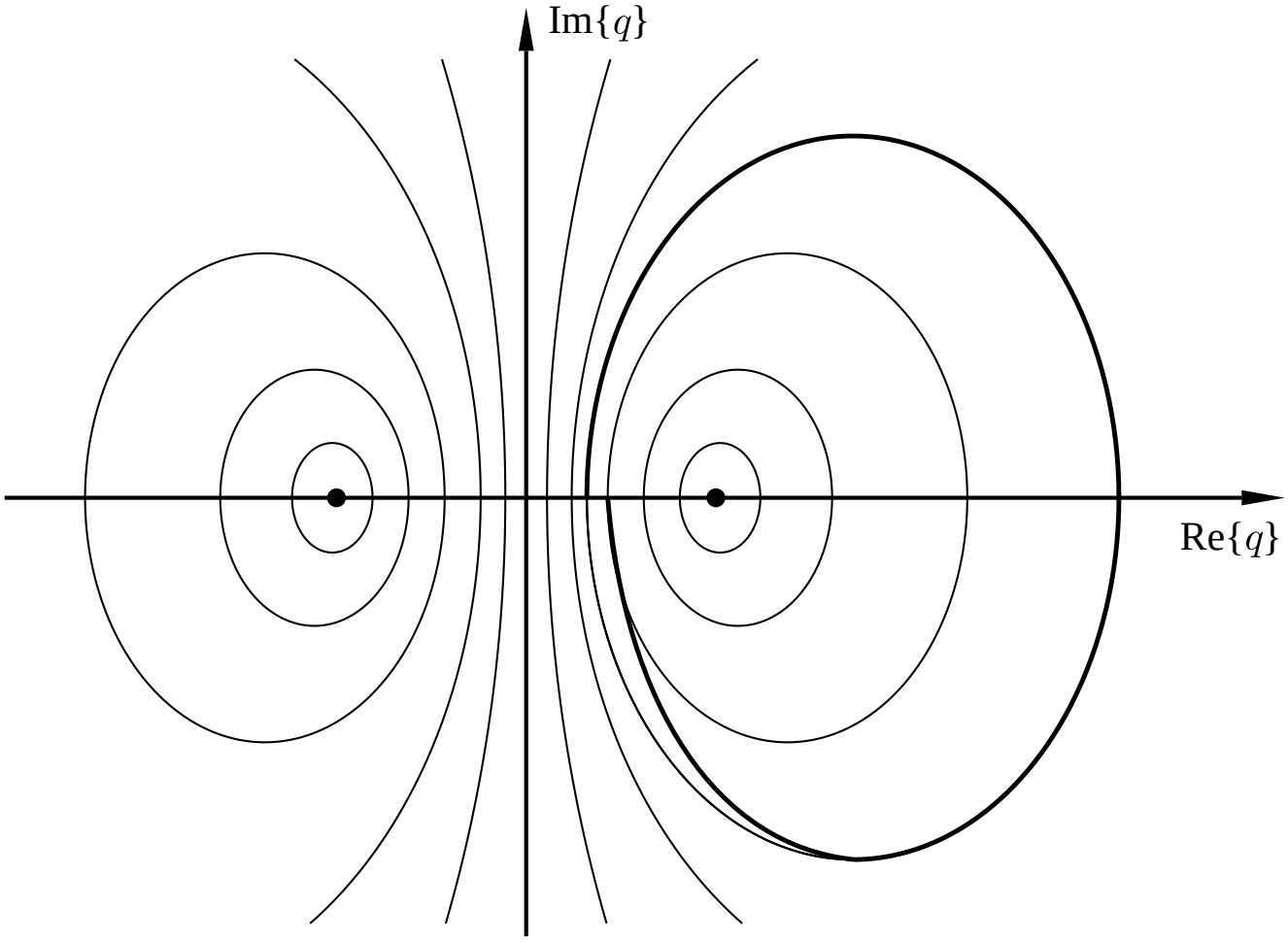

Figure 3, Ankerhold et al.

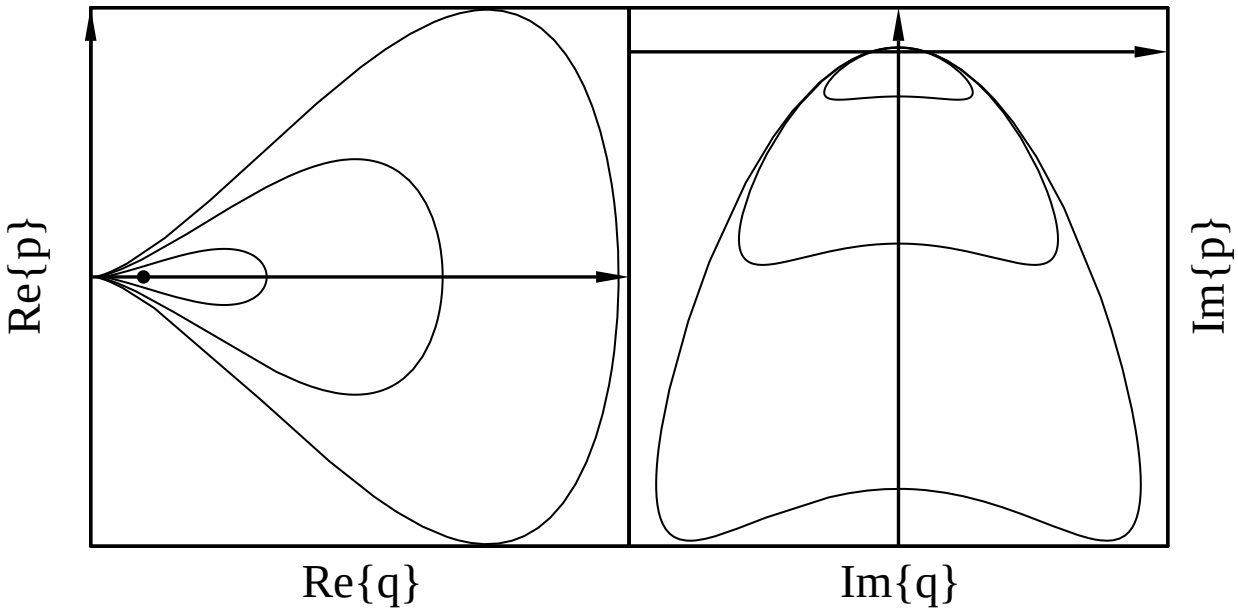

Figure 4, Ankerhold et al.

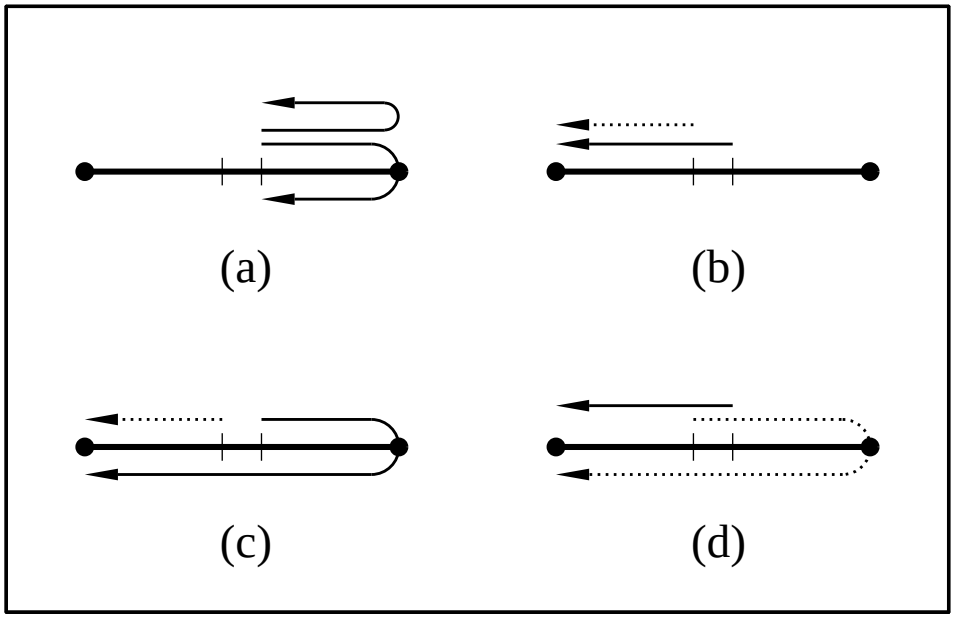

Figure 5, Ankerhold et al.

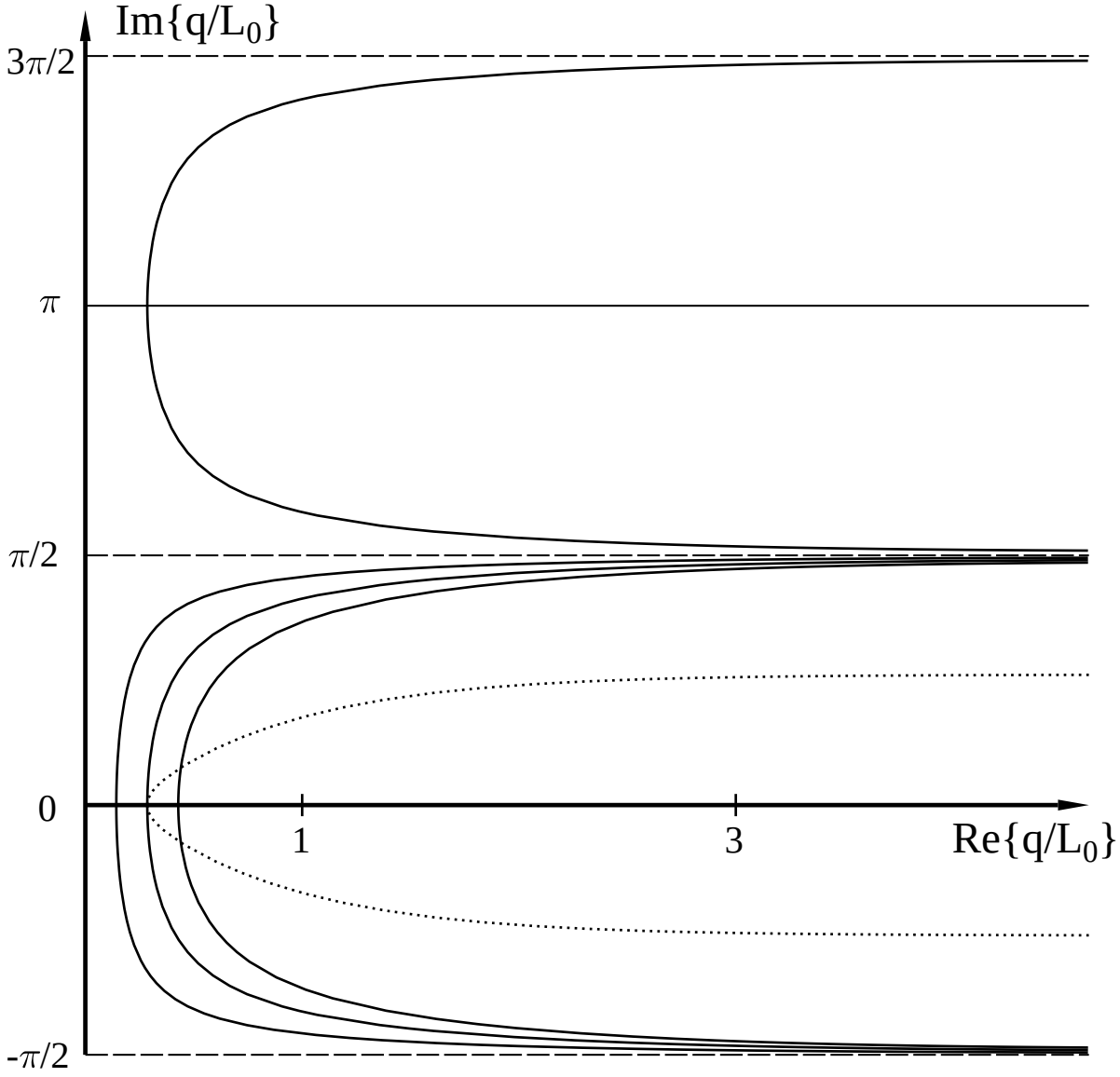

Figure 6, Ankerhold et al.

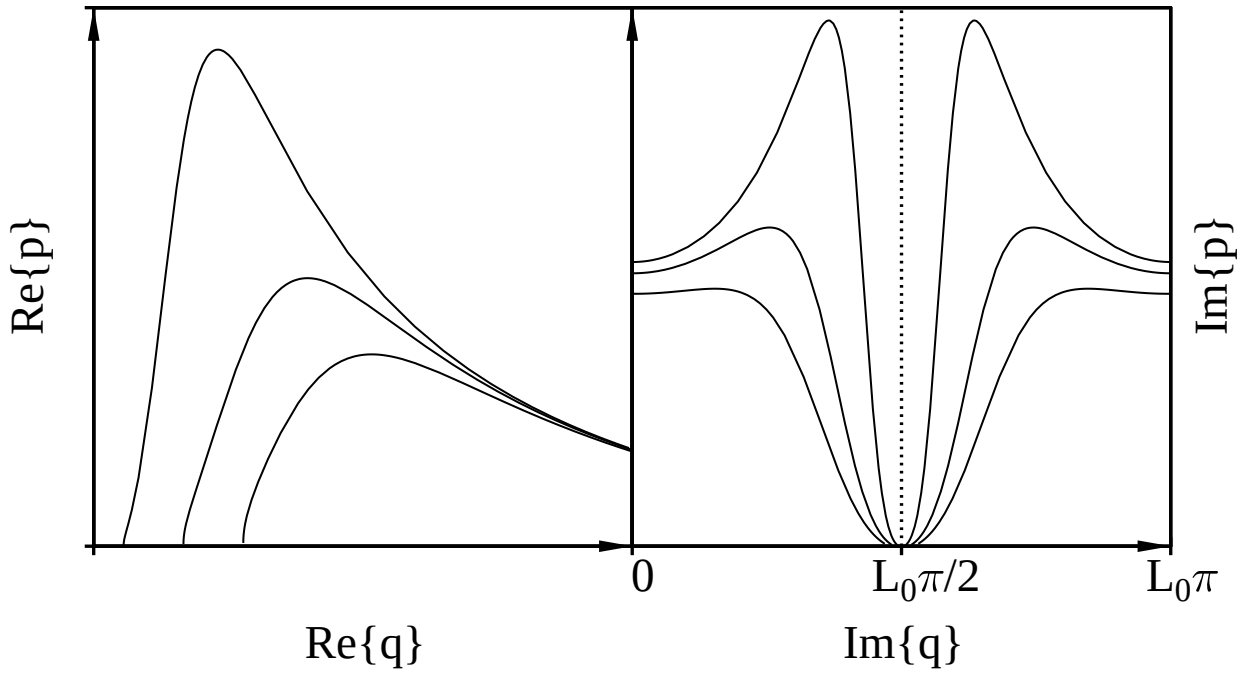

Figure 7, Ankerhold et al.

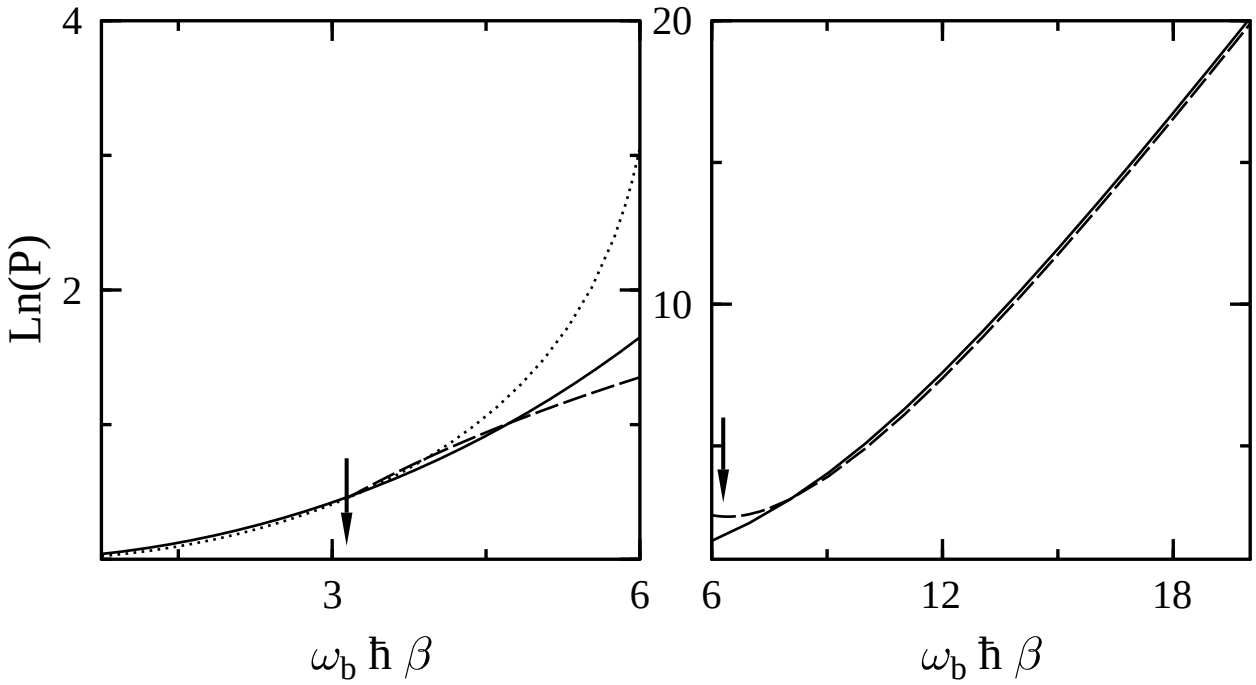

Figure 8, Ankerhold et al.